Stabilization and Characterization of Bi(III) Compounds with *peri*-substituted AcenaphtheneBased Ligands

A Thesis

submitted to

Indian Institute of Science Education and Research Pune in partial fulfilment of the requirements for the M.Sc. Degree Programme

By

Ankan Kundu

(20226208)

Indian Institute of Science Education and Research PuneDr.

Homi Bhabha Road,
Pashan, Pune 411008, INDIA.

March, 2024

Supervisor: Dr. Moumita Majumdar

Student: Ankan Kundu

Certificate

This is to certify that this dissertation entitled **Stabilization and Characterization of Bi(III) Compounds with *peri*-substituted Acenaphthene Based Ligands** towards the partial fulfilment of the M.Sc. degree programme at the Indian Institute of Science Education and Research, Pune represents research work carried out by **Ankan Kundu** (20226208) at Indian Institute of Science Education and Research under the supervision of **Dr. Moumita Majumdar**, Associate Professor, Department of Chemistry, during the academic year 2023- 2024.

Moumita Majumdar

Dr. Moumita Majumdar

Supervisor

Committee:

Supervisor: Dr. Moumita Majumdar

TAC: Dr. Sujit Ghosh

This thesis is dedicated to my family, friends and my lab partners

Declaration

I hereby declare that the matter embodied in the report entitled **Stabilization and Characterization of Bi(III) Compounds with *peri*-substituted Acenaphthene Based Ligands** are the results of the work carried out by me at the Department of Chemistry, Indian Institute of Science Education and Research, Pune, under the supervision of Dr. Moumita Majumdar and the same has not been submitted elsewhere for any other degree.

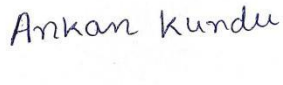

Ankan Kundu

Date: 01/05/2024

Table of Contents

List of Tables

List of Schemes

Abbreviations

Ace	Acenaphthene
*i*Pr	iso-propyl
Ph	Phenyl
Me	Methyl
n-BuLi	n-butyl lithium
DCM	Dichloromethane
THF / thf	Tetrahydrofuran
tht	Tetrahydrothiophene
$CDCl_3$	Deuterated chloroform
OTf	Triflloromethanesulphonate
AgOTf	Silver Triflourumethanesulphonate
COD	1,5-cyclooctadiene
TMS	Tetramethyl silane
g	grams
mg	mili grams
eq.	equivalent(s)
δ	Chemical shift
MHz	Megahertz

Abstract

Sigma acceptor ligands play a crucial role in transition metal catalyzed lewis acid catalysis. The presence of such ligands around the transition metal center can significantly tune the nature of lewis acidity of the transition metal, leading to exceptional catalytic activity. There are some handful reports on group 14 elements for such ligands. In our work, we have utilized *peri*- substituted acenaphthene framework to prepare these ligands using group 15 element i.e. bismuth. Herein we have synthesized bismuth based neutral complexes (**1**, **5**, **7**) by employing one, two and three equivalents of 6-diphenylphosphinoacenaphth-5-yl and 6-diisopropylphosphinoacenaphth-5-yl ligands. Exploring the nature of these neutral complexes, chlorine atom abstraction from the bismuth center have been performed, resulting in generation of compounds **2**, **3** and **6**. These compounds have been investigated throughly using single crystal X-ray diffraction and NMR analysis. We have performed the reactions using these ligands and transition metal complexes and reported the possible formation of cu complex (**4**) of bismuth monocationic compound (**3**).

Acknowledgement

I want to express my sincere gratitude to my thesis supervisor Dr. Moumita Majumdar for giving me the opportunity to work in her lab and providing me a great lab atmosphere for my research. Her exceptional guidance and support throughout my MS thesis were pivotal in shaping my academic journey.

I am also grateful to my TAC member Dr.Sujit Ghosh for his invaluable feedback and suggestions, which greatly contributed to the enhancement of my research work. I would also like to thank my all lab members Ms. Purba Chibde, Mr. Akash Waghmare, Mr. Rahul Deb, Mr. Niranjan Patel, Ms. Nilanjana Mukherjee, Mr. Souvik Khan, Ms. Akanksha Kumari, Ms. Diya Sengupta, Ms. Jasmita Bhoi, Mr Hritwik Halder, Mr. Satyabrata Das and Mr. Upal Pramanik for their friendly attitude and moral support throughout the journey.

I would like to thank the Department of Chemistry at IISER Pune for providing an outstanding research opportunities along with access to the excellent NMR and XRD facilities. I also want to thank my family and friends for their continuous support during the challenging phases of my academic pursuit. Lastly, I appreciate the INSPIRE for their financial support which plays a crucial role in facilitating my academic endeavors.

1. Introduction:

1.1. Introduction of group 15 Lewis acids :

Main group compounds have shown potential to replace transition metal complexes in synthetic chemistry and catalysis because of being less toxic and showing transition metal-like reactivity in cationic or neutral state. The overall physical and chemical properties of a chemical center are invariably altered when charge is introduced. Generally, main-group cationic species tend to show noticeably higher Lewis acidity compared to their underlying neutral compounds. Similarly, anionic species demonstrates enhanced lewis basicity/ nucleophilicity in comparison to neutral counterparts.[1,5] However, in the context of group 15 elements, stark differences are observed in properties of the heavier pnictogens (Sb, Bi) and their lighter congeners (N, P, As). Accessibility of higher co-ordination being one of the noticeable properties. The reason being size of the elements and their electronegativity. Down the group, the size of the atoms increases, making them accessible for more co-ordination as the steric crowding between the attaching groups decreases considerably. The second reason is the electropositivity of the elements. Down the group, the electronegativity of the elements decreases. As a result, the interaction with the nucleophiles increases. Hence, the heavier elements are able to form hexa or higher coordinated compounds.[1,2,6] The heavier p-block compounds based on Sb, Bi act as lewis acceptors alike transition metal complexes. For the element bismuth, being non-radiative, heaviest and its extreme position in the periodic table (6th period), the lewis accepting characteristics have been less explored. The very large, diffuse and polarizable valence orbital of bismuth, high energy gap between s and p orbital and decrease in one electron ionization energy (I_1) makes huge difference in the bonding situations in the heavier pnictogens.[3] Nevertheless the transformation of neutral bismuth(III) compound into well-established cationic moieties, has developed as an promising strategies with interesting bonding situations and reactivity pattern.

Generally, removal of a monoanionic ligand (such as aryls, amides, alcoholates or hallides) from a neutral bismuth(III) compounds [BiR_3] generates cationic bismuth compound [BiR_2]$^+$ which contains a vacant p-orbital on the bismuth centre, a weakly coordinating counter anion and a occupied s-orbital on bismuth centre.

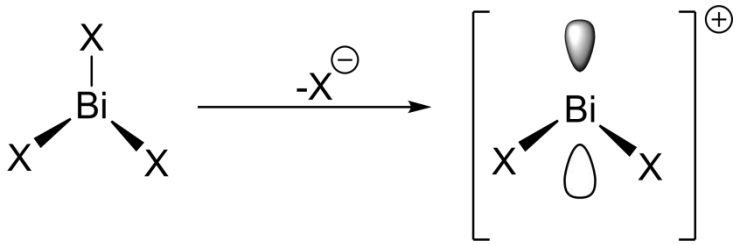

Fig. 1: Orbital diagram of monocationic bismuth species.

The available p-orbital on the bismuth atom can take part in intra- and intermolecular σ and π type bonding situations and plays a crucial role in redox chemistry as well as lewis acid catalysis. The vacant orbital allows aggregation effects, lewis acidic activation of external substrates, also changes the energy of frontier orbitals.[4] Also introducing mono or higher positive charges on a acceptor centre increases its lewis acidity.

The lewis acidic bismuth (III) centre can be classified into three different classes A-C (as shown in fig 2). The compounds of class A are not cationic species. Their lewis acidity is a result of the antibonding σ* Bi-X orbital which is normally available for interactions with the lewis bases when X atom is sufficiently electronegative. Class C are the types of compounds that are cationic in nature, where the cationic centre and the anion does not interact. In this class, the compounds form lewis base adduct with the vacant p-orbital of [R_2Bi]$^+$ moiety. Class C are the intermediate compounds of class A and C, where the Bi- -X bonding interaction are weak in nature as the negative charge delocalizes in X (where X = O_3SCF_3, $AlCl_4$).[5]

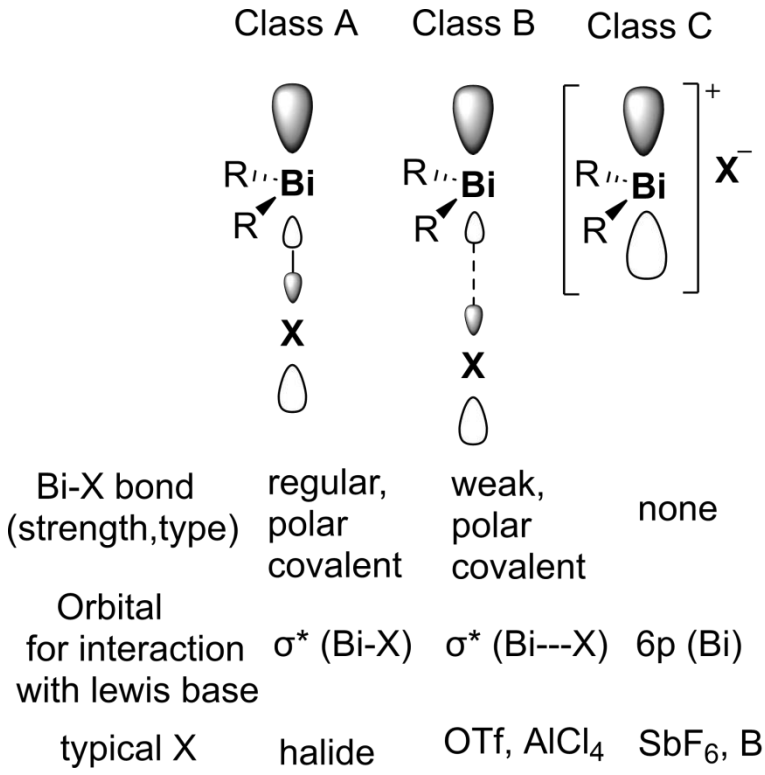

Fig. 2: Orbital picture of three classes(A-C) of bismuth lewis acids.

The bismuth lewis acid can be utilised to selectivities and activities which are diificult to obtain with any other reagents.[1] For every classes of bismuth lewis acids, the orbital involved in the interactions with lewis bases are large and diffuse, which indicates that they are soft lewis acids.[7]

Recently in 2020 Lichtenberg *et al* have synthesized the cationic bimepine with olefin bridge in the ligand backbone (compound 1) which preferentially binds with soft donors i.e. phosphane chalcogenides $EPMe_3$ (E=S, Se) by replacing two hard thf ligand with 87% and 91% yield. This indicates that the transfer of electron density from the soft bases or donors to the vacant 6p orbital of bismuth stabilizes the lewis acidic bismuth centre. Here, the olefin bridge present in the ligand backbone reduces the flexibility of the aryl groups in compound 1 and provides some steric repulsion at the bismuth centre. So, more strerically demanding EPMe3 group forms a 1:1

stoichiometric lewis acid/base adduct in compound 1 whereas, 2 equivalent of thf forms an adduct with the bismuth atom.

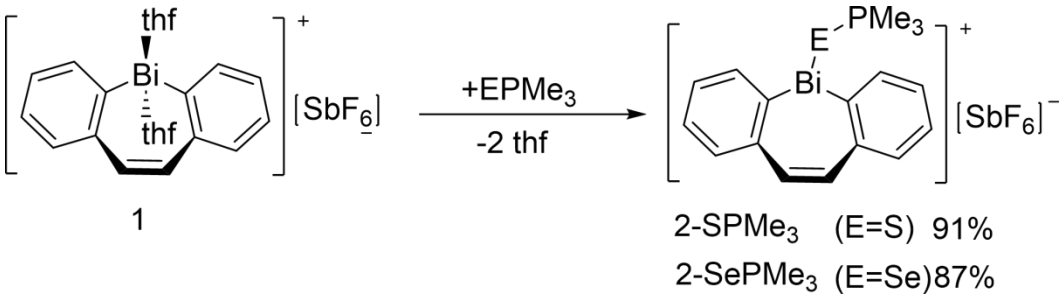

Fig. 3: Reaction of cationic bismepine 1 with soft donors $EPMe_3$ to give **2-EPMe$_3$** through thf elimination (E=S, Se).

Beckmann *et al* in 2018 synthesized bismuthenium and stibenium ion (figure 4) where the cationic centre is surrounded by bulky meta-terphenyl substituents and the weakly coordinating borate anion which remains outside the co-ordination sphere. Contrary to the previously reported diaryl bismuth and diaryl antimony salts where inter- or intramolecular donor atom co-ordination (Fig 3) or co-ordination of the counter anion to the metal centre is observed,[37] no such coordination is observed in this case.

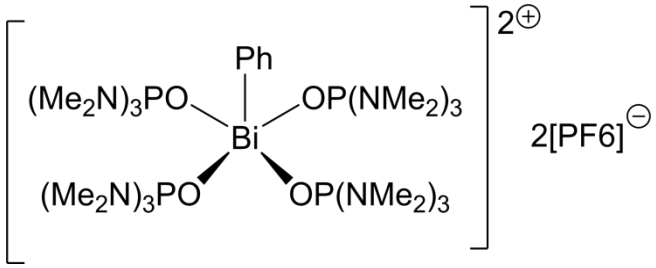

Fig. 4: Di-cationic bismuth centre stabilized via donation of electron density from oxygen to the vacant orbital of bismuth.

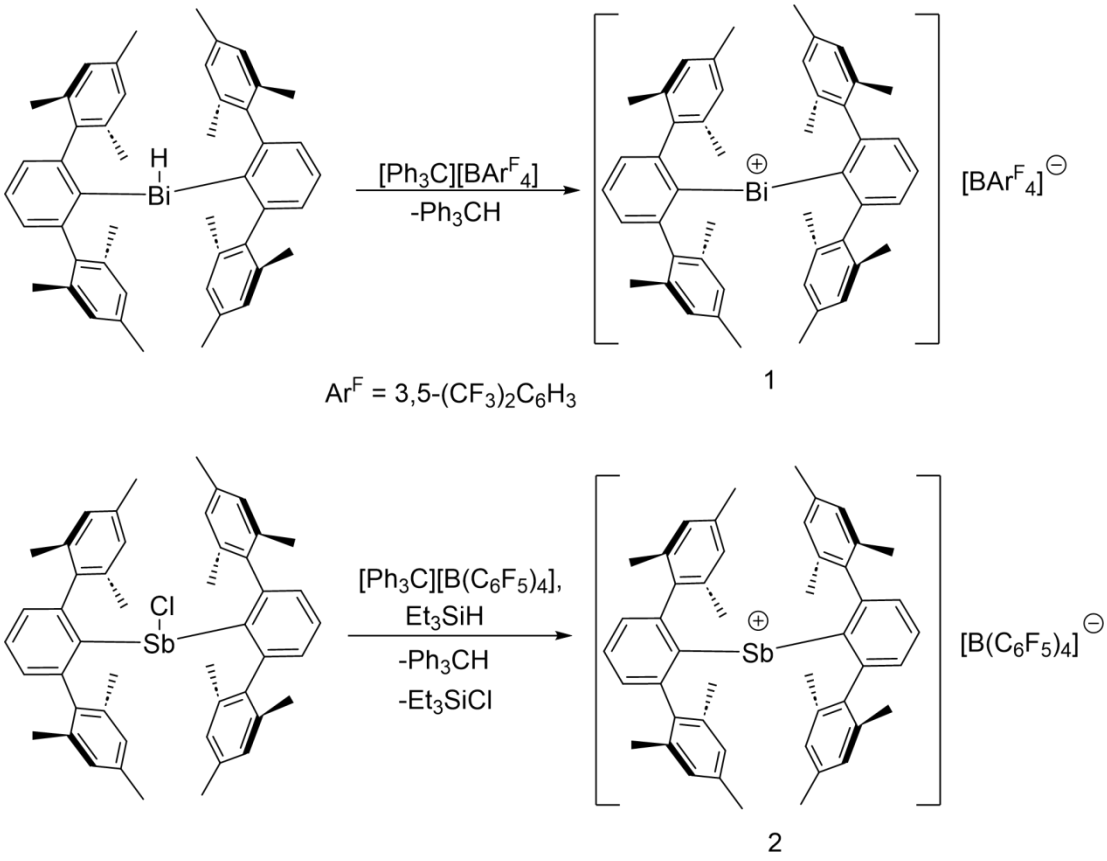

Fig. 5: Synthesis of Bismuthenium ion 1 and stibenium ion 2.

In the above two examples of bismuthenium and stibenium ions, the steric hindrance provided by two bulky ligand substituent protects the reactive cationic centre from undergoing dimerization or being attacked by the counter anion. This is an example of kinetic stabilization. While kinetically stabilized heavier congeners of carbene R_2E (E = Si, Ge, Sn, Pb) are known, but reports of iso-electronic group 15 cation of the $[R_2E]^+$ (E = Sb,Bi) type are scarce.[8]

1.2. The role of the weakly coordinating anion :

As we are discussing the cationic compounds, the bonding situations can be altered by the nature of the counter anion. The example of such anions that show this bonding interactions are $[OTf]^-$, $[BAr^F_4]^-$, $[B(C_6F_5)_4]^-$, $[BF_4]^-$, $[AlCl_4]^-$, $[ClO_4]^-$ etc. The lewis acidity of the class B compounds i.e. $[BiR_2(L)_n(WCA)]$ and class C compounds i.e. $[BiR_2(L)_n][WCA]$ (Fig 2), can be accessed by the LUMO of the corresponding class of compounds, which results in the interactions with the lewis bases.

The LUMO shows major contributions of sigma* (Bi---WCA) for $[BiR_2(L)_n(WCA)]$ compounds and unoccupied bismuth p orbital for $[BiR_2(L)_n][WCA]$ compounds.[4] Also the stability of the WCA is an important factor to deal with. If the cationic species is highly electrophilic in nature, it shows high tendency to co-ordinate with an anion which may be abstracted from the WCAs. This leads to the degradation by heterolytic cleavage of a bond in these counter anions.[9]

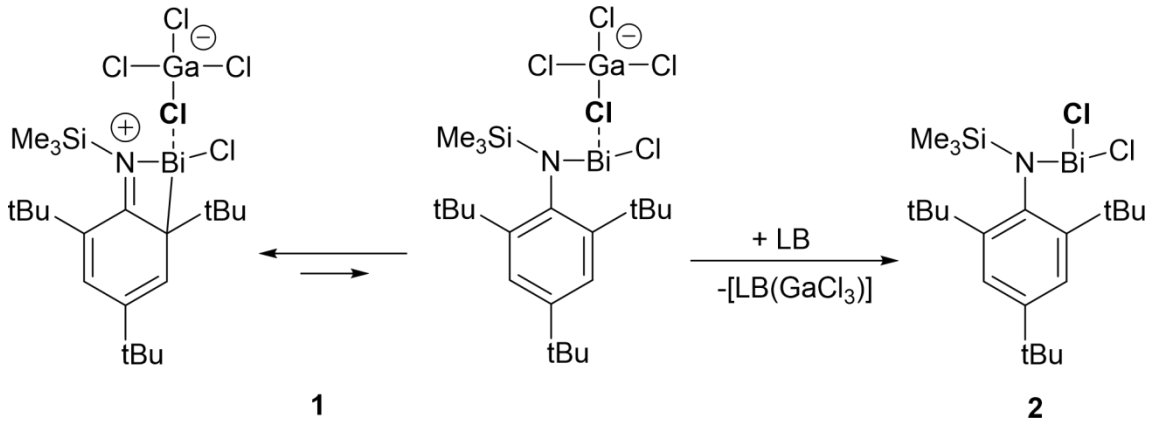

Fig. 6: Degradation of WCA in presence of cationic bismuth compound.

Despite of these problems there are many advantages that allow to choose suitable WCA (Fig 7) to stabilize the reactive bismuth cations.[10]

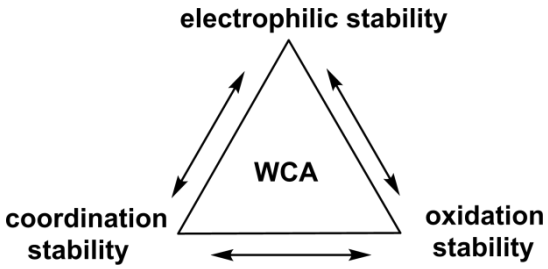

Fig. 7 : The demands of WCA in stabilizing reactive cations.

1.3. Introduction of group-15 Z- type ligand :

The compounds that generally accepts two electrons from the metal centre are called Z-type ligand (BR3, AlR3, GaR3 etc). The lewis acidic compounds mainly act as Z-type ligands. In X-type ligand both the metal centre and the ligand donates one electron each to form a bond (H, Cl, Me radicals etc). Whereas in L-type the ligand donates two electrons to the metal centre (I.e. CO, NH3, PR3 etc).

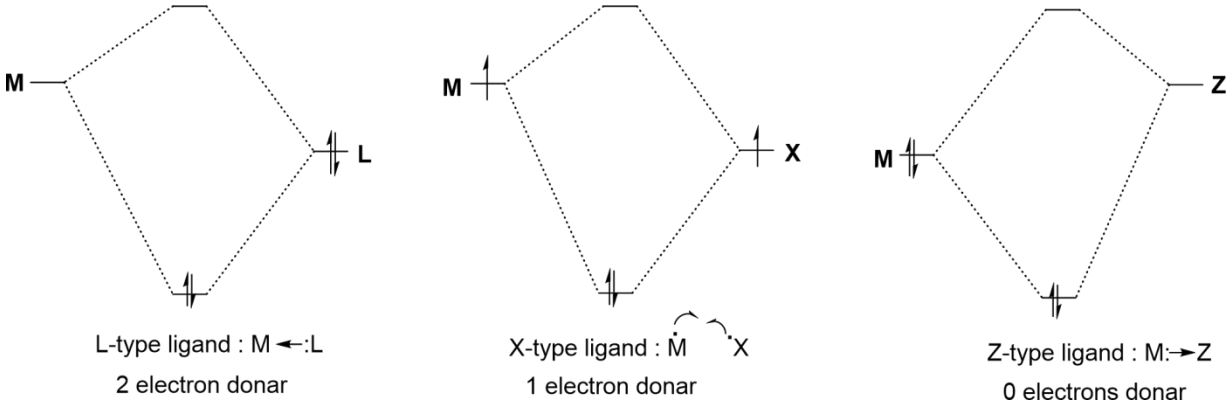

Fig. 8: Three classes of ligand system

At first, the concept of Z-type ligand was introduced for group-13 compounds, mainly for boranes. This is because these elements have an unoccupied p orbital that can form a strong sigma interaction with the filled d-orbital of the transition metal center. Hill and co-workers in 1999 synthesized Ruthenaboratrane complex where the Pd center sufficiently donates the electron density to the lewis acidic boron moiety.[11]

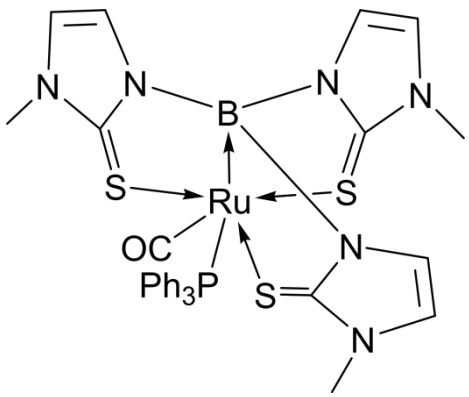

Fig. 9 : Synthesis of Ruthenaboratrane complex where Boron center acts as a Z-type ligand.

Bourissou *et al* in 2007 synthesized the gold co-ordinated diphosphanylborane compound where the gold center is donating electron density towards the boron center. Here the resulted Au→B complex forms a square-planar, which confirms the d^8 Au (III) geometry in this system (fig 10). The two phosphane moiety in the ligand system and gold center adopts slightly bent geometry trans to the boron center. This evidence strongly supports that the metal co-ordination occurs only in the trans geometry of the ligand.[12]

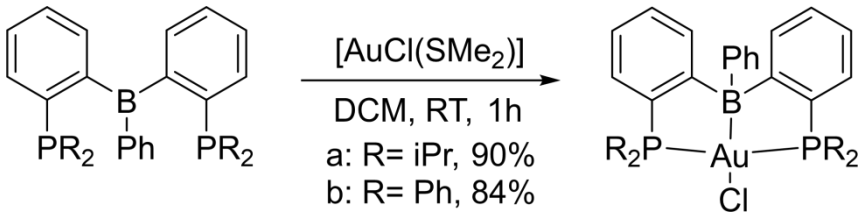

Fig. 10: Co-ordination of AuCl to amphibilic diphosphanylborane compound.

In the last two decades, there are many reports of group 14 elements (Si, Ge, Sn) acting as Z-type ligand. [13-17] Among group 15 elements, although there are some reports of antimony forming Z-type ligand[18-23], the reports of bismuth acting as a Z-type ligand are very rare.[23,24,25] This is because of the fact that down the group the electropositivity of the elements increases significantly, bismuth being the heaviest element it has the lesser tendency to pull the electron density from the coordinated metal center and exhibit as a Z-type ligand. Secondly, bismuth being soft lewis acid, it accepts electron density from the coordinated redox-active transition metal center and converts Bi(III) to Bi(0) as a black precipitate.

In 2011, Gabbaï and group reported the complex 1-Cl i.e. [(o-$(PPh_2)C_6H_4)_3$SbAuCl] (Fig.11) where there is a weak donor-acceptor interaction from the Sb lone pair to the vacant p-orbital of Au center. Upon oxidizing the Sb(III) center in complex 1-Cl to Sb(V) in compound 2 by $PhICl_2$, the umpolung in the Au-Sb dative bond was found and subjected as lp(Au)→**σ***(Sb-Cl). This complex 2 acts as a Z-type ligand. Also the Au-Sb bond becomes more stronger in complex 2 than 1-Cl. But the complex 2 does not undergo reversible reaction by strong reducing agents. Then they converted the

complex 2 into 1-I by NaI and the compound 1-I can easily re-oxidized by $PhICl_2$ and excess nBu_4NCl.[22]

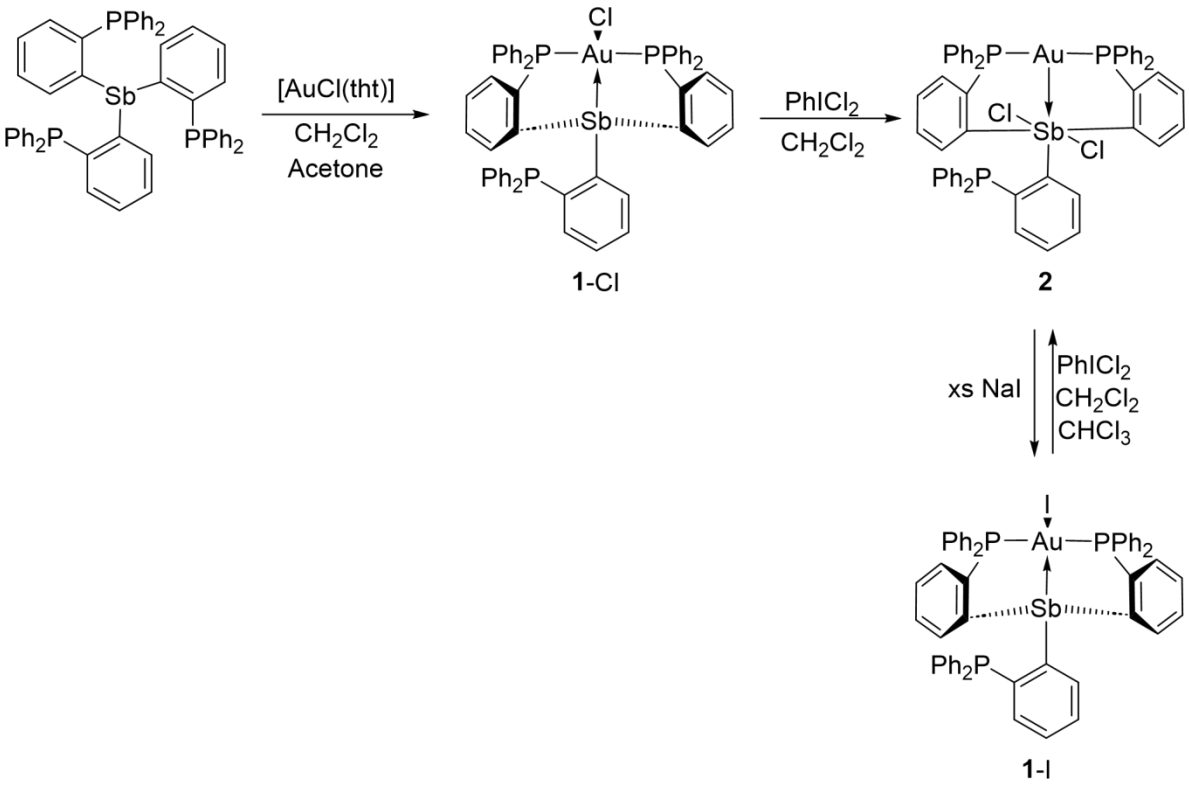

Fig. 11: The reversible process induces umpolung of the Sb-Au bond.

In 2015, Gabbaï *et al* reported the complex [3][SbF_6] which is an example of Z-type ligand (Fig.12), where the oxidation state of the Sb center plays a major role in catalytic activity. At first, they synthesized the complex 1-Cl. Then they treated the complex 1-Cl with $AgSbF_6$ to obtain compound [1][SbF_6]. But both the complexes 1-Cl and [1][SbF_6] exhibited very low catalytic activity. Then they combined the complex 1-Cl with $PhICl_2$ to convert Sb(III)center to Sb(V) (compound 2-Cl). Due to solubility issue of the compound 2-Cl, they converted this compound into 3-Cl and abstracting the chlorine atom from the gold center generated the compound [3][SbF_6]. The Au→Sb donor-acceptor interaction is strongest in the complex [3][SbF_6] as the lewis acidity of the Sb(V) center increases significantly and acts as a efficient catalyst for hydroamination of terminal alkynes.[18]

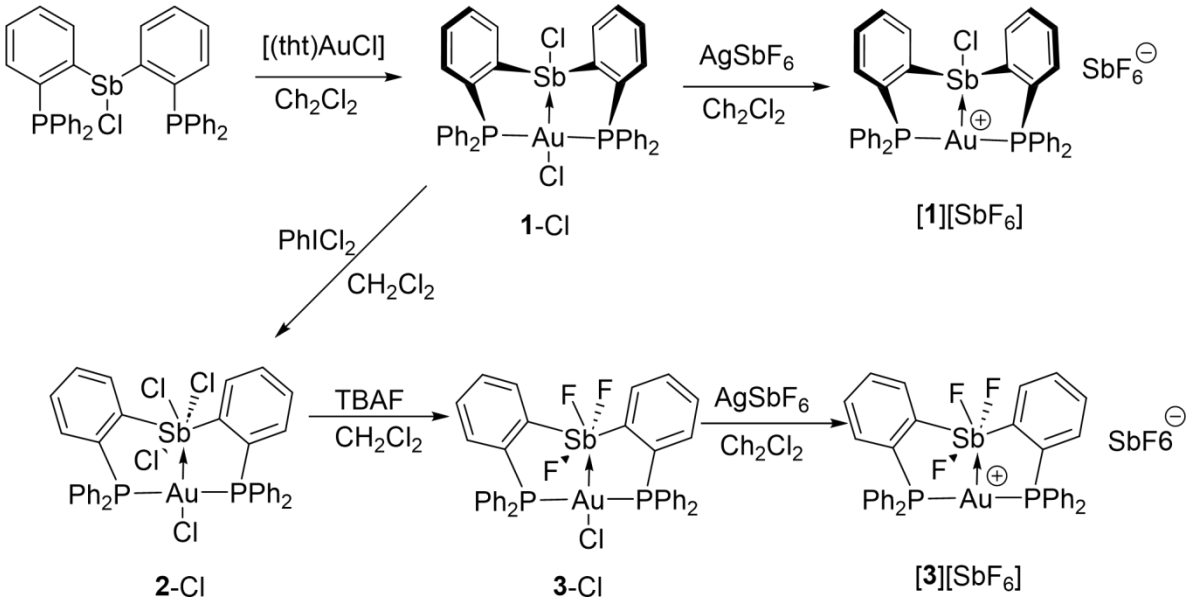

Fig. 12: Synthesis of active catalyst [3][SbF_6].

Gabbaï and group in 2019 synthesized an antimony(V) di-cationic complex ([3][NTf_2]$_2$) which acts as a Z-type ligand (Fig.13). The goal of synthesizing such complex was to demonstrate the effect of charge on Z-type ligand, which can tune the electrophilic as well as the catalytic activities of the coordinated gold center. At first, they have oxidized the previously reported compound 1,[22] by hydrogen peroxide to obtain compound 2 ([2a][Cl]). After adding 2 eq. of $AgNTf_2$, the compound [3][NTf_2]$_2$ obtained, which is stabilized via the intra-molecular donation of electron density from the phosphine oxide. The Au-Sb bond lengths in these compound 2 and 3 are significantly shorter than the compound 1, indicating the lewis acidity at the Sb center increases. When another equivalent of $AgNTf_2$ was added to the compound [3][NTf_2]$_2$, the compound [4][NTf_2]$_2$ generated, where the Cl atom at the gold center is replaced bt the weakly coordinating NTf anion. The compound [4][NTf_2]$_2$ acts as an active catalyst for the activation of styrene and hydroamination reactions. Thus the di-cationic Sb(V) Z-type ligand coordinated to the gold center facilitates such reactivites.[21]

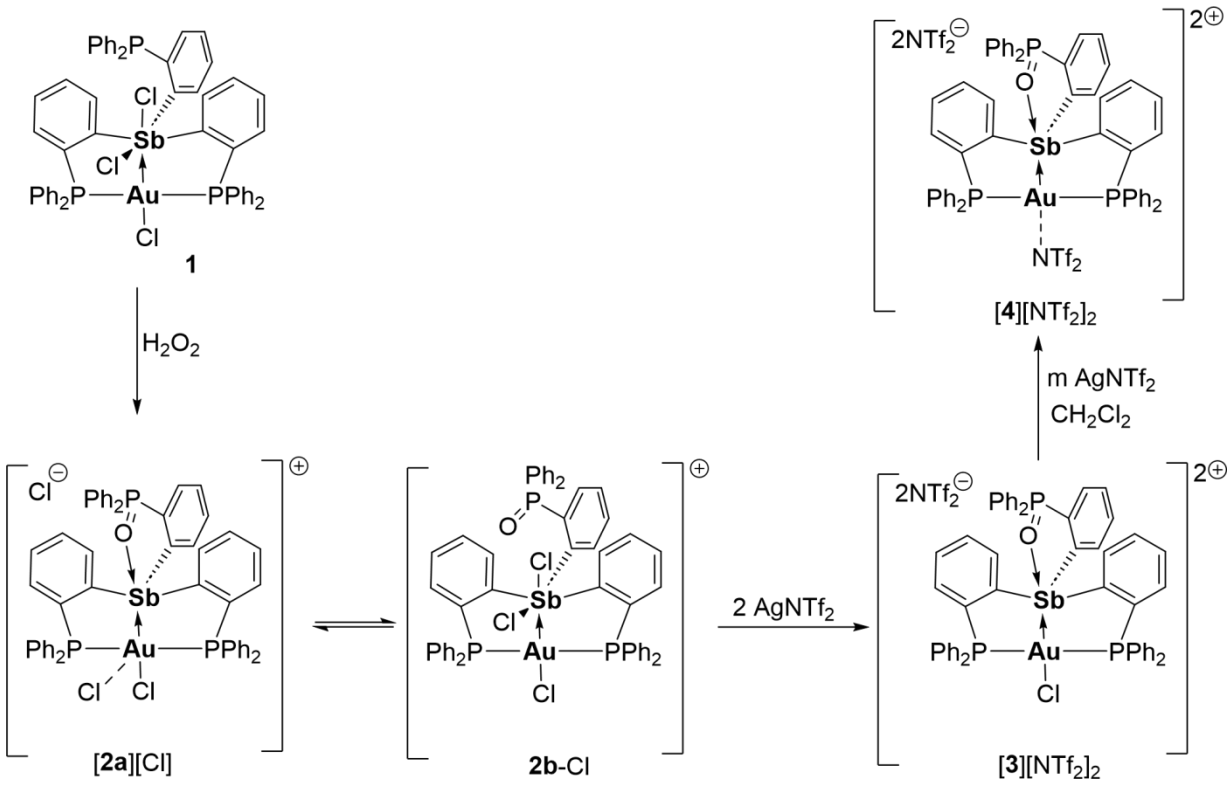

Fig.13: Synthesis of di-cationic Sb(V) complex co-ordinated to gold center.

Gabbaï *et al* in 2018 synthesized the antimony-platinum complex, where the donation of electron density occurs from the platinum to antimony center. They reacted the previously reported complex 1,[18] with TlF and donar ligands to afford compound 2 and 3 (Fig.14). The bond length in compound 2 and 3 elongates and becomes more polarized (dative), whereas the Sb-Pt bond was covalent in compound 1. Although the bond become polarized, the donation of electron density from the platinum to antimony center is not sufficient, where as in compound 4 (obtained by fluoride atom abstraction from compound 2 and 3) the platinum center becomes more electrophilic in nature. They found the compound 4 and 5 are active catalyst for the cyclization of 1,6-enyne.[19]

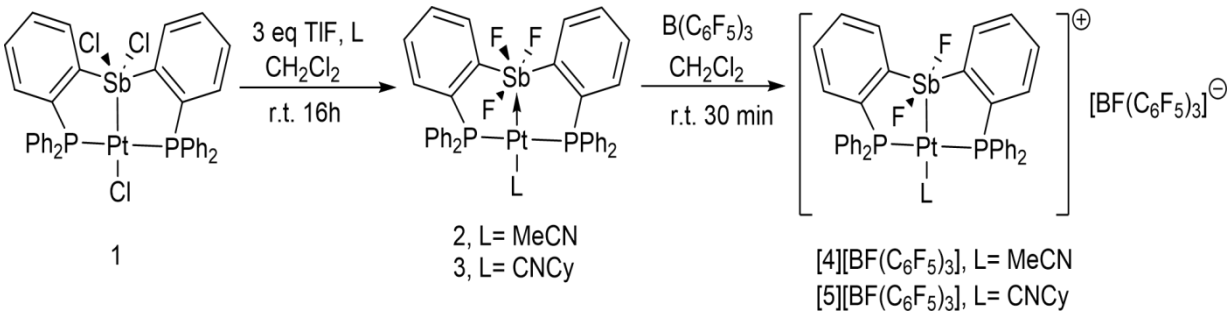

Fig. 14: Synthesis of active catalyst for enyne cyclization.

Limberg and group synthesized gold and platinum coordinated Bismuth complex in 2012, where the bismuth center is acting as a Z-type ligand (fig 15). To stabilize such M→Bi (M = Au,Pt) interactions they used the amphibilic ligand framework, where both the lewis acidic bismuth center and the lewis basic phosphane donors are present. The lewis acidic bismuth center accepts the electron density from the filled $5d_{x2-y2}$ and 5d orbital of the corresponding Au and Pt center.[25] To obtain compound 2, they at first lithiate the compound 1 followed by addition of BiCl3. Then addition of [Au(PPh3)Cl] and [Pt(cod)Cl_2] to the compound 2, they obtained the following heterometallic complexes 3 and 4.

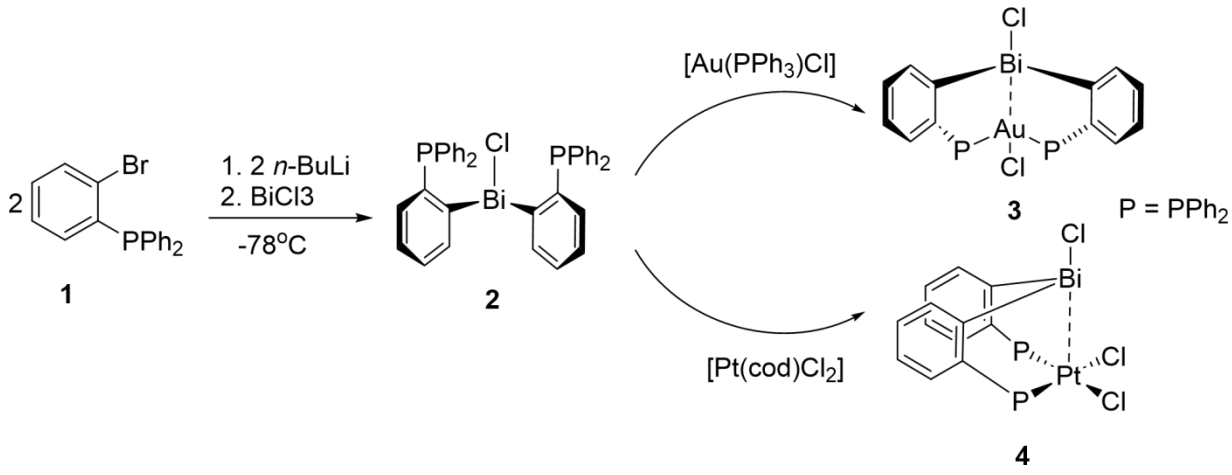

Fig.15: Synthesis of gold and platinum co-ordinated heterometallic complexes 3 and 4, where cod = 1,5-cyclooctadiene.

In this work, we have synthesized *peri*-substituted acenaphthene based ligands 6-diphenylphosphinoacenaphth-5-yl- and 6-diisopropylphosphinoacenaphth-5-yl. The ligands are employed both in one, two and three equivalents as -R groups to

stabilize bismuth based neutral and mono-cationic compounds. Using these types of ligands we wanted to see how the rigid backbone of the acenapthene and different electronic features containing phosphines [electronic acceptor phosphines (-PPh2) and electron donar phosphines (-PiPr2)] are tuning the electronic features of bismuth mono-cationic center and their lewis acidic character. Further bis(6-diphenylphosphinoacenaphth-5-yl-) and bis(6-diisopropylphosphinoacenaphth-5-yl-) ligand stabilized bismuth(III) neutral and monocation compounds can be used as a Z-type ligands[23,25] for stabilizing transition metal based compounds where phosphines coordinate to transition metal centre and lewis acidic bismuth(III) centre accepts electron density from transition metal.

2. Materials and method

2.1. Equipment and Experimental materials

All manipulations were carried out under a protective atmosphere of argon applying standard Schlenk techniques or in a dry box. Tetrahydrofuran (THF) was refluxed over sodium/benzophenone. Dichloromethane (DCM) and acetonitrile (MeCN) were stirred and refluxed over calcium hydride and kept over 3 Å molecular sieves. All solvents were distilled and stored under argon and degassed prior to use. CDCl3 was dried, distilled and stored under argon and degassed prior to use. All chemicals were used as purchased.1H and 13C{1H} NMR spectra were referenced to external SiMe4 using the residual signals of the deuterated solvent (1H) or the solvent itself (13C). 19F{1H} and 31P{1H} NMR were referenced to external C6H5CF3 (TFT) and 85% H3PO4 respectively. NMR spectra were recorded on Bruker AVANCE III HD ASCEND 9.4 Tesla/400 MHz, Jeol 9.4 Tesla/400 MHz and Bruker AVANCE III HD ASCEND 14.1 Tesla/600 MHz. Single crystal data were collected on both Bruker SMART APEX four-circle diffractometer equipped with a CMOS photon 100 detector (Bruker Systems Inc.) with a Cu K radiation (1.5418 Å), and Bruker SMART APEX Duo, Bruker APEX-II CCD diffractometers using Mo K radiation (0.71073 Å).

2.2. Preparations:

2.2.1. Synthetic procedure of 5,6-dibromoacenapthene:

Acenapthene (10 g, 64.8 mmol) and N-bromo succinimide(28.84 g, 162 mmol) were mixed in 70 ml of DMF solvent and stirred for 24 hours at room temparature. The N-bromo succinimide compound was weighed in dark atmosphere as it is sensitive to light. After 24 hours white colour precipitate was obtained at the bottom of the RB flask. To eliminate the liquid solvent, the precipitate was filtered out and repeatedly washed with chilled methanol. Then, by recrystallization from hexanes, this crude product was purified. The yield of the product is around 25-30%.

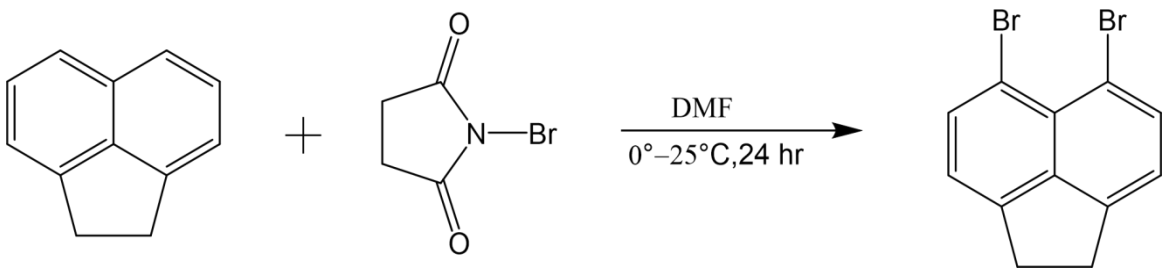

Scheme 1. Synthesis of 5,6-dibromo-acenaphthene.

^{1}H NMR (400 MHz, in $CDCl_3$, 298K) δ 7.12-7.03 (d, j = 7.46, 2H); 7.82-7.76 (d, j = 7.46, 2H); 3.29 (s, 4H) ppm.

2.2.2. Synthetic Procedure of 5-Bromo,6-phosphino-acenaphthtene (L^{iPr}-Br & L^{Ph}-Br):

Synthesis of L^{iPr}-Br:

5,6-Dibromoacenaphthene (6.00 g, 19.2 mmol) was dissolved in tetrahydrofuran (THF) (100 ml) and cooled to -78°C. n-BuLi (12.0 ml of 1.6 M solution in hexane, 19 mmol) was added dropwise to it, maintaining -78°C and stirred for 2 hours at the same temperature. Chlorodiisopropylphosphine (3.0 ml, 19.2 mmol) taken in THF (25 ml) was added dropwise to the resultant mixture maintaining -78°C. The solution mixture was then allowed to warm to room temperature and stirred overnight. The solvent was removed completely by evaporation and toluene was added to the solid residue. The toluene solution was separated from the suspended solid through filtration. The toluene extract was completely evaporated to give 5-Bromo,6-(diisopropylphosphino)acenaphthene L^{iPr}-Br as yellow solid in 76% (5.1 g) yield.

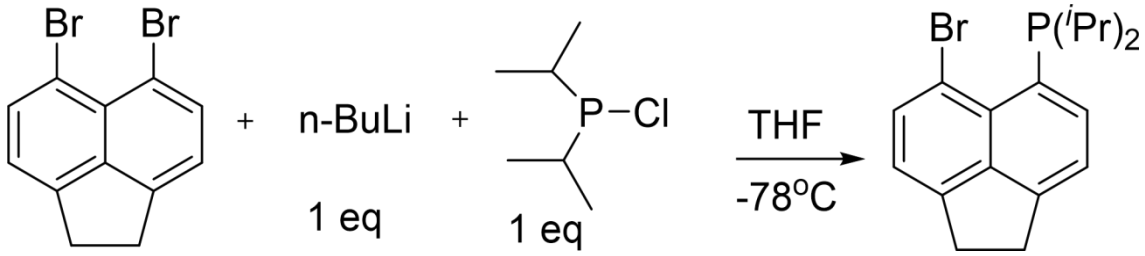

Scheme 2. Synthesis of 5-Bromo,6-diisopropylphosphino-acenaphthtene.

^{1}H NMR (400 MHz, in CDCl3, 298K) δ 7.78 (d, *J* = 7.4 Hz, 1H), 7.69 (dd, *J* = 7.3, 2.5 Hz, 1H), 7.30 (dt, *J* =7.2, 1.4 Hz, 1H)), 7.10 (dt, *J* = 7.4, 1.4 Hz, 1H), 3.33 (s, 2H), 3.36 (s, 2H), 2.23 (pd, *J* = 7.0, 2.0 Hz, 2H), 1.19 (dd, *J* = 12.8, 6.9 Hz, 6H), 1.07 (dd, *J* = 13.4, 7.0 Hz, 6H) ppm.

^{13}C {^{1}H} NMR (400 MHz, in CDCl3, 298K) δ 148.00, 147.05, 141.67, 135.37, 134.92 (d, *J* = 2.3 Hz), 134.10 (d, *J* = 18.6 Hz), 130.28 (d, *J* = 34.0 Hz), 120.33, 119.69, 115.63, 30.01 (d, *J* = 40.2 Hz), 25.60 (d, *J* = 17.8 Hz), 20.68 (d, *J* = 15.4 Hz), 19.34 (d, *J* = 16.3 Hz) ppm.

^{31}P {^{1}H} NMR (400 MHz, in CDCl3, 298K) δ -2.11 (s) ppm.

Synthesis of L^{Ph}-Br:

5,6-Dibromo acenaphthene (4.50 g, 14.4 mmol) was dissolved in THF (100 ml) and cooled to -78 °C. n-BuLi (9.0 ml of 1.6 M solution in hexane, 14.4 mmol) was added dropwise to it maintaining -78 °C and stirred for 2 hours at the same temperature. Chlorodiphenylphosphine (2.6 ml, 14.4 mmol) taken in THF (25 ml) was added dropwise to the resultant mixture maintaining -78 °C. The solution mixture was then allowed to warm to room temperature and stirred overnight. The solvent was removed completely by evaporation and dichloromethane (DCM) was added to the solid residue. The DCM solution was separated from the suspended solid through filtration. The DCM extract was completely evaporated to give 5-Bromo,6-(diphenylphosphino) acenaphthene **L^{Ph}-Br** as yellow solid. Yellow crystals of **L^{Ph}-Br** have been obtained in 52% yield (3.1 g) from concentrated DCM solution.

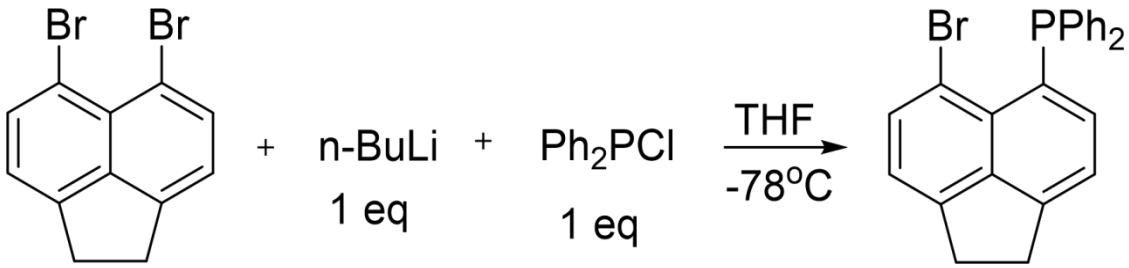

Scheme 3. Synthesis of 5-Bromo,6-diphenylphosphino-acenaphthtene.

^{1}H NMR (400 MHz, in CDCl3, 298K) δ 7.71 (d, J = 7.4 Hz, 1H), 7.32 (m, 6H), 7.29 (m, 4H), 7.12 (m, 2H), 7.08 (d, J = 4.4 Hz, 1H), 3.34 (s, 4H, Acn-CH2) ppm.

^{13}C{1H} NMR (400 MHz, in CDCl3, 298K) CDCl3) δ 148.67 (s, Acn-C), 146.93 (d, J = 2.0 Hz, Acn-C), 141.71 (d, J = 4.1 Hz, Acn-C), 139.35 (d, J = 14.2 Hz, Acn-CH), 138.01 (s, Acn-C), 134.84 (s, Acn-CH), 134.32 (d, J = 20.1 Hz, Acn-C), 133.49 (d, J = 18.6 Hz, Ph-CH), 130.11 (d, J = 33.3 Hz, Ph-C), 128.64 (d, J = 6.8 Hz, Ph-CH), 128.55 (s, Ph-CH), 120.85 (s, Acn-CH), 120.40 (s, Acn-CH), 115.97 (s, Acn-CBr), 30.28 (s, Acn-CH2), 30.04 (s, Acn-CH2) ppm.

^{31}P{1H} NMR (400 MHz, in CDCl3, 298K) CDCl3) δ -9.29 (s) ppm.

2.2.3. Synthetic procedure of [L^{Ph}_2BiCl] (L^{Ph}=6-diphenylphosphinoacenaphth-5-yl) (**1**): 5-Bromo,6-(diphenylphosphino) acenaphthene **L^{Ph}** (1 equivalents) was dissolved in THF (30 ml) and cooled to -78 °C. n-BuLi (1 equivalents, 1.6 M solution in hexane) was added dropwise to it maintaining -78°C and stirred for 2 hours at the same temperature. $BiCl_3$ (0.5 equivalents) taken in THF (10 ml) was added drop wise to the resultant mixture maintaining -78 °C. The solution mixture was then allowed to warm to room temperature and stirred overnight. The solvent was removed completely by evaporation and dichloromethane was added to the solid residue. The dichloromethane solution was separated from the suspended solid through filtration. The dichloromethane extract was evaporated completely to give crude solid. The crude solid was dissolved in minimum volume of DCM. Colorless single crystals of **1** were obtained from concentrated DCM solution maintained at room temperature in 60% yield.

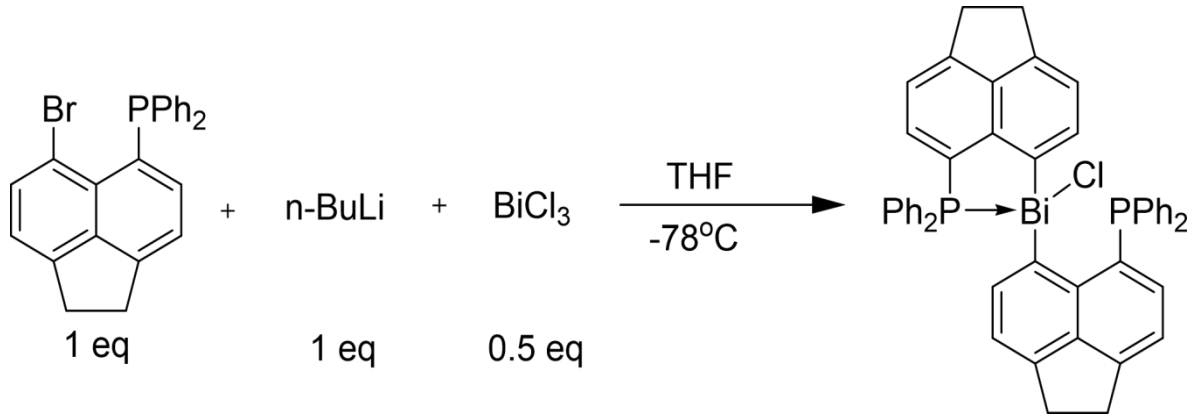

Scheme 4: Synthesis of **[L_2^{Ph} BiCl] (1)**

^{1}H NMR (400 MHz, in CDCl3, 298K) δ 9.18-9.13 (s, 1H); δ 7.22-7.07 (m, 27H); δ 3.35 (s, 8H) ppm.

^{31}P {^{1}H} NMR (400 MHz, in CDCl3, 298K) δ -21.81 (s) ppm.

2.2.4. Synthetic Procedure [L^{Ph} $BiCl^{+}$](OTf^{-}) (L=L^{Ph}=6-diphenylphosphinoacenaphth-5-yl) (**2**) :

One equivalent of **[L^{Ph}_2-BiCl] (1)** was dissolved in 10 ml of DCM and then solid AgOTf (1 equivalent) was added in the solution. The reaction mixture was stirred for overnight. The solution was filtered and the filtrate was concentrated and kept for crystallization at room temperature. Colorless single crystals of **2** obtained by slow diffusion of n-pentane into DCM solution at room temperature within 5 days.

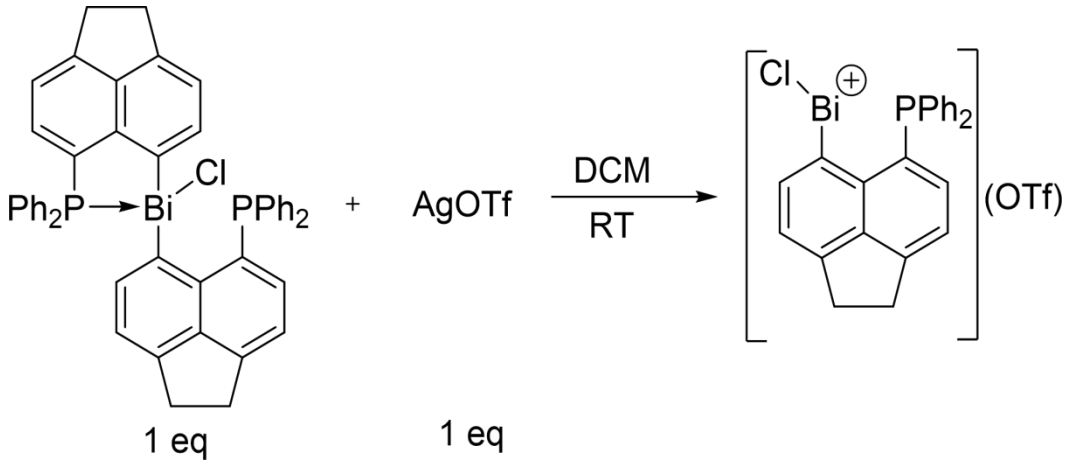

Scheme 5: Synthesis of [L^{Ph}-$BiCl^{+}$][OTf^{-}] **(2)**

2.2.5. Synthetic procedure of **[$L^{Ph}_2$$Bi^+$][$OTf^-$]** [$L^{Ph}$=6-diphenylphosphinoacenaphth-5-yl) (**3**) :

One equivalent of **[L_2^{Ph}-BiCl]** (**1)** was dissolved in 10 ml of DCM and then TMSOTf (1 equivalent) was added in the solution. The reaction was stirred for overnight at room temperature. Then the solvent was removed completely by vacuum evaporation and THF was added. A yellow coloured solution obtained after filtration, which was kept for crystallization at room temperature. Colorless single crystals of **3** obtained within two days. The compound was characterized by X-ray diffraction analysis.

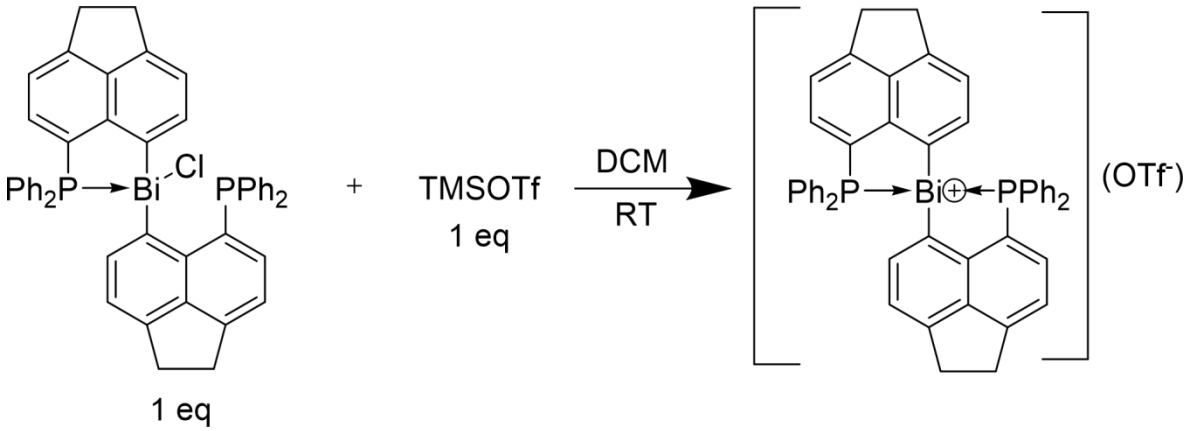

Scheme 6 : Synthesis of **[L_2^{Ph}-Bi^+][OTf^-] (3)**

^{1}H NMR (400 MHz, in CDCl3, 298K) δ 8.39-8.32 (d, J = 7.1 Hz, 1H), 7.69-7.61 (dt, J = 7.8 Hz, 1H), 7.57-7.35 (m, 25H), 7.33-7.28 (d, J = 7.21,1H), 3.34-3.18 (m, 8H) ppm.

^{13}C{1H} NMR (400 MHz, in CDCl3, 298K) δ 153.53 (s, Acn-C), 147.86 (s, Acn-C), 147.15 – 147.04 (m, Acn-C), 143.32 (s, Acn-C), 142.8 – 142.26 (m, Acn-CH), 142.48 (s, Acn-C), 137.26 (s, Ph-CH), 133.86 (s, Ph-C), 129.69 (s, Acn-CH), 129.46 – 129.35 (m, Ph-CH), 129.05 (s, Ph-CH), 128.23 (s, Acn-CH), 125.30 (s, Acn-CH), 124.78 – 124.66 (m, Acn-C), 121.14 (s, Acn-CH), 31.5 (s, Acn-CH2), 31.19 (s, Acn-CH2) ppm.

^{19}F{1H} NMR (400 MHz, in CDCl3, 298) δ -77.95 (s) ppm.

^{31}P{1H} NMR (400 MHz, in CDCl3, 298K) δ 7.90 (s) ppm.

2.2.6. Synthetic procedure of **[L^{Ph}_2 Bi(+)]** co-ordinated CuCl complex [L^{Ph}=6 diphenylphosphinoacenaphth-5-yl) (**4**) :

One equivalent of **[L_2 ^{Ph}-Bi(+)]** (**3)** and CuCl (1 equivalent) were dissolved in 5 ml DCM and 3 ml acetonitrile solution respectively in two different vials. Then the two solutions were added in a 25 ml schlenk RB. The reaction mixture was stirred for overnight at room temperature. Then the solvent was removed completely by vacuum evaporation and the obtained yellow residue was washed with acetonitrile solution (2 ml). Then the residue was dried in vacuum and DCM was added to it. The obtained compound **4** was characterized by ^{31}P NMR spectroscopy.

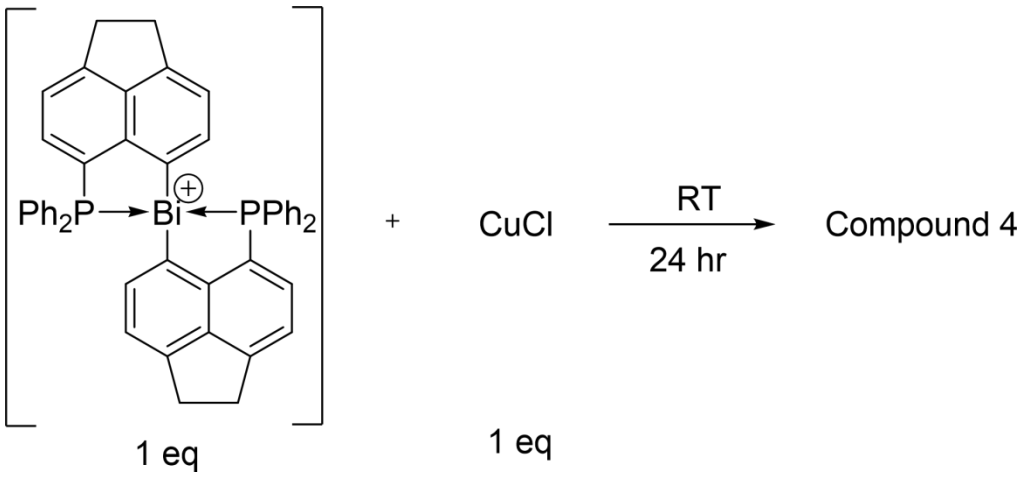

Scheme 7: Reaction of compound **3** with CuCl.

^{31}P {^{1}H} NMR (400 MHz, in CDCl3, 298K) δ 40.32 (s) ppm.

2.2.7. Synthetic Procedure of **[L^{ipr}-BiCl$_2$]** (L^{ipr} = 6-diisopropyl-phosphino-acenaphth-5- yl) (**5**) :

5-Bromo,6-(diisopropylphosphino)acenaphthene L^{ipr}-Br (1 equivalent) was dissolved in THF (50 ml) and cooled to -78 °C. n-BuLi (1 equivalent, 1.6 M solution in hexane) was added dropwise to it maintaining -78 °C and stirred for 2 hours at the same temperature. $BiCl_3$ (1 equivalent) taken in THF (20 ml) was added dropwise to the resultant mixture maintained at -78 °C. The solution mixture was then allowed to warm to room temperature and stirred overnight. The solvent was removed completely by evaporation and dichloromethane (DCM) was added to the solid residue. The dichloromethane solution was separated from the suspended solid through filtration. The dichloromethane extract was evaporated completely to give crude yellow solid. The crude yellow solid was dissolved in minimum volume of DCM. Colorless single crystals of **5** were obtained from concentrated DCM with pentane layering maintained at room temperature in 75% yield. Detailed crystal structure is shown below.

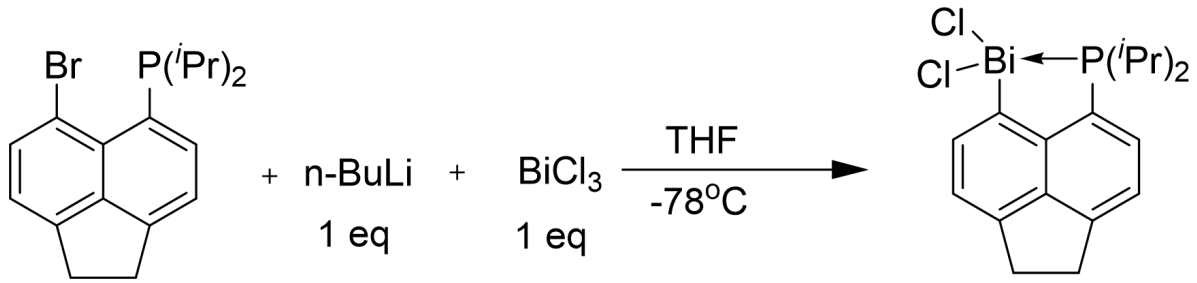

Scheme 8. Synthesis of [L^{ipr}-BiCl$_2$] (**5**).

2.2.8. Synthetic Procedure of **Ag-Cluster** (L=L^{Ph}=6-diphenylphosphinoacenaphth-5-yl) (**6**) :

One equivalent of **[L^{ipr}-BiCl$_2$]** (**5**) was dissolved in 10 ml of DCM and then solid AgOTf (1 equivalent) was added in the solution. The reaction mixture was stirred for 4 hours. The solution was filtered and the filtrate was concentrated and kept for crystallization at room temperature. Colorless single crystals of **6** obtained by slow diffusion of n-pentane into DCM solution at room temperature after 3 days.

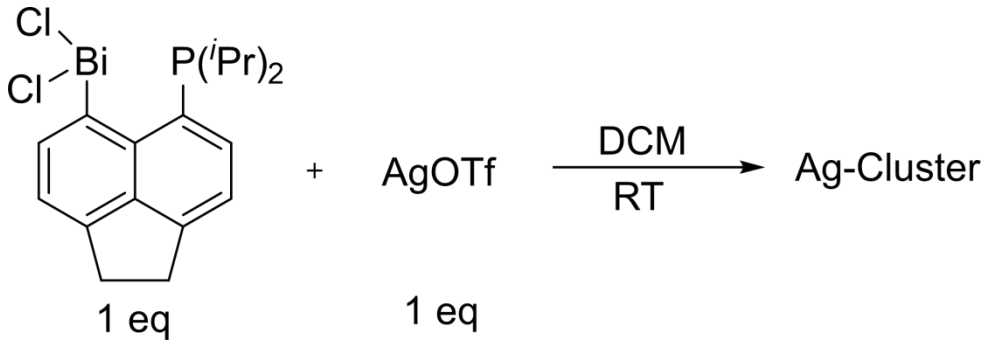

Scheme 9 : Synthesis of Ag-Cluster **(6)**

2.2.9. Synthetic Procedure of **[L$^{iPr}_3$Bi]** (L^{ipr} = 6-diisopropyl-phosphino-acenaphth-5-yl) (**7**):

5-Bromo,6-(diphenylphosphino) acenaphthene **L^{iPr}-Br** (3 equivalents) was dissolved in THF (30 ml) and cooled to -78 °C. n-BuLi (3 equivalents, 1.6 M solution in hexane) was added drop wise to it maintaining -78°C and stirred for 2 hours at the same temperature. $BiCl_3$ (1 equivalent) taken in THF (10 ml) was added drop wise to the resultant mixture maintaining -78 °C. The solution mixture was then allowed to warm to room temperature and stirred overnight. The solvent was removed completely byevaporation and dichloromethane was added to the solid residue. The dichloromethane solution was separated from the suspended solid through filtration. The dichloromethane extract was evaporated completely to give crude solid. The crude solid was dissolved in minimum volume of DCM. Colorless single crystals of **7** were obtained from concentrated DCM solution maintained at room temperature in 32% yield.

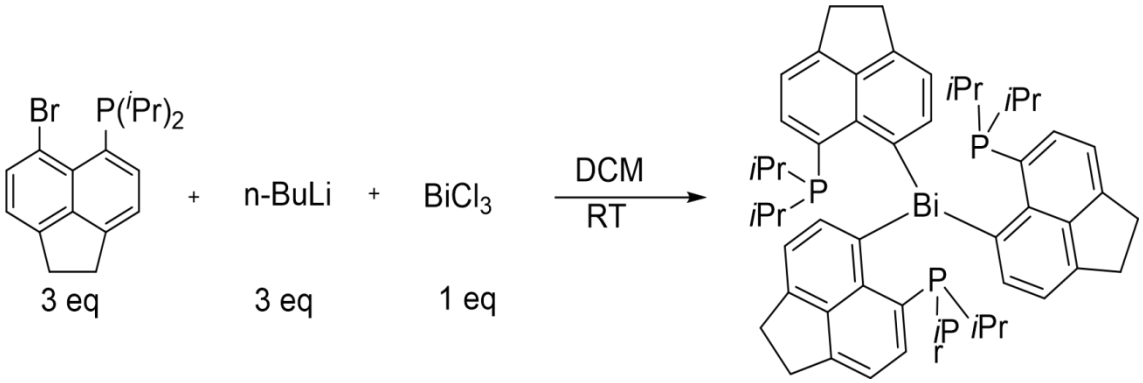

Scheme 10: Synthsis of **[L$^{iPr}_3$BiCl] (7)**

^{31}P {^{1}H} NMR (400 MHz, in CDCl3, 298K) δ -21.29 (s).

3 Results and discussion:

Syntheses and their charecterization:

The precursor for the ligand, 5,6-dibromoacenaphthene was synthesized by the reaction of acenaphthene with N-bromo succinimide (NBS) in DMF solvent following the literature procedure[26]. The two ligand framework **L^{iPr}-Br** & **L^{Ph}-Br** were synthesized by the reaction of 5,6-dibromoacenaphthene with n-BuLi at -78°C to generate the lithiated intermediate and butyl bromide(n-BuBr). Subsequent addition of $(iPr)_2PCl$ and Ph_2PCl after two hours gives rise to the 5-Bromo,6-diisopropylphosphino-acenaphthtene(**L^{iPr}-Br)** and 5-Bromo,6-diphenylphosphino-acenaphthtene (**L^{Ph}-Br)**[26,27]. The single crystals of **L^{Ph}-Br** were obtained from DCM solution as brown coloured within two days. Then the crystals were washed with n-pentane solution and dried in vaccum.The ligand **L^{Ph}-Br** were charecterized using single crystal X-ray diffraction analysis and ^{1}H, ^{13}C and ^{31}P NMR analysis and the ligand **L^{iPr}-Br** were charecterized by ^{1}H, ^{13}C and ^{31}P analysis.

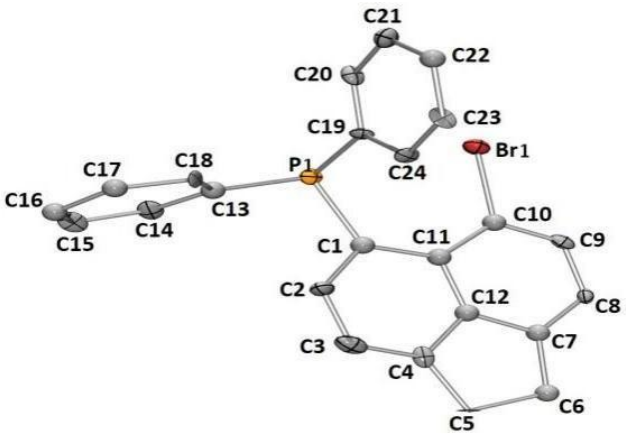

Fig. 16: crystal structure of the Ligand **L^{Ph}-Br** (thermal ellipsoid at 30% probability, H atoms are excluded for clarity)**.**

The compound **1** i.e. [$L^{Ph}{}_2$ BiCl] was obtained by the reaction of 5-bromo,6-diiphenylphosphino acenaphthene(L^{Ph}-Br) (1 eq) and 0.5 equivalents of $BiCl_3$. The single crystals of compound **1** were grown from DCM/n-pentane solutions as yellowish brown colour and characterized by single crystal X-ray diffraction analysis (SC-XRD) and ^{1}H, ^{31}P NMR analysis.

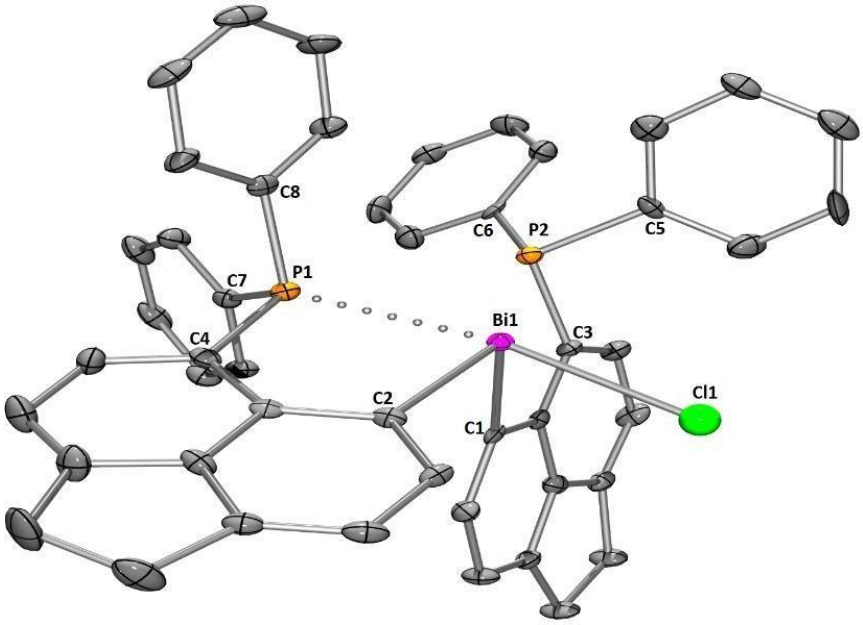

Fig. 17: Crystal structure of the Compound **1** (thermal ellipsoid at 30% probability, H atoms are excluded for clarity). The selected bond lengths [Å] and bond angles [°]: Bi1-Cl1 = 2.800(1), Bi1-P1 = 2.826(1), Bi1-P2 = 3.262, Bi1-C1 = 2.265(6), Bi1-C2 = 2.274(7), P1-C4 = 1.797(7), P2-C3 = 1.828(7).

The compound **1** crystallizes in triclinic P1 space group containing the [$L^{Ph}{}_2$BiCl] and three non-coordinating DCM solvent molecules in the asymmetric unit (Fig.17, Table 1). Here in the molecular structure of the compound **1** the one of the Bi-P bond length (Bi1-P1 = (2.826(1) Å) is much shorter than the sum of their vanderwaal's radius (Σ_{rvdW}(Bi-P) = 3.87 Å), indicating there is a significant interaction between the bismuth and phosphorus center. The P1 center present at the trans of the Bi1-Cl1 bond donates the electron density to the anti-bonding orbital of the Bi1-Cl1 bond. As a result the Bi1-Cl1 bond becomes longer (Bi1-Cl1 = 2.800(1)Å) than their covalent radii ($\Sigma_{r,cov}$(Bi-Cl) = 2.5 Å). Also there is some sort of back-donation from the filled $6s^2$

orbital of the Bi atom to the P center. This is also supported from ^{31}P NMR analysis where we can clearly see the δ value is shifted from -9.29 ppm (for compound L^{Ph}- Br) to more upfield i.e -21.81 ppm. This confirms the fact that the electron density around phosphorus center increases.

To increase the lewis acidity of the bismuth center we moved to the formation of the cationic species of compound **1**. This mono-cationic compound can act as a Z-type ligand like Gabbaï *et al* reported carbenium ion acting as a Z-type ligand where the donation of electron density occurs from the filled d-orbital of gold center to the acridinium or xanthenium moiety[32]. To investigate the interesting chemistry of this cationic complex and its possibility to act as a Z-type ligand, we were highly enthusiastic about exploring the potential of this complex **2** to coordinate with the transition metals. To obtain the cationic complex **2**, [L^{Ph}_2 -BiCl] (compound **1**) and AgOTf were combined in 1:1 molar ratio. Colourless single crystals of the compound **2** were grown from DCM/n-pentane solution and the compound was characterized by single crystal X-ray diffraction analysis, which confirms the formation of the product **2**.

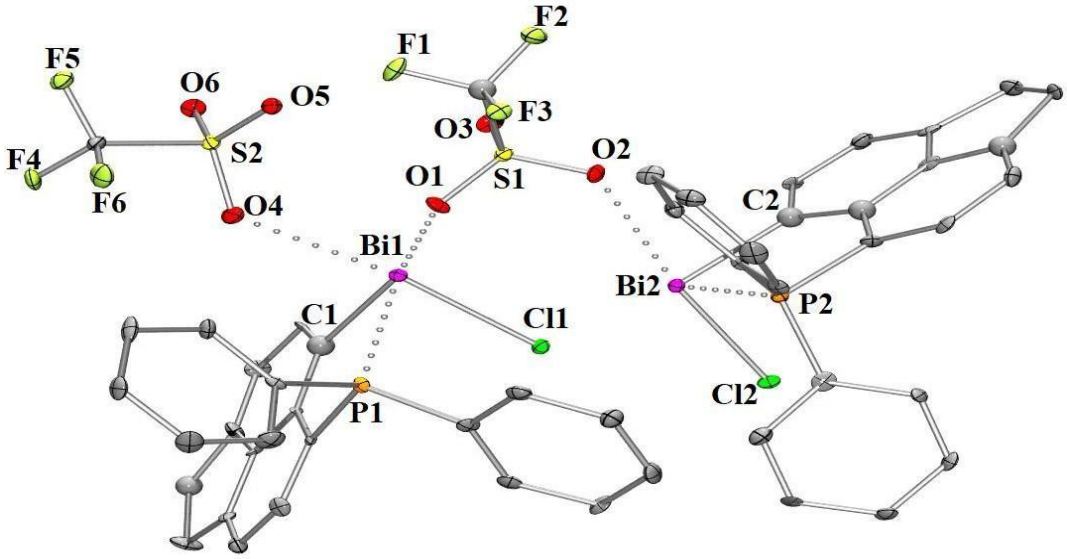

Fig. 18: Crystal structure of the Compound **2** (thermal ellipsoid at 30% probability, H atoms are excluded for clarity).The selected bond lengths [Å] and bond angles [°]: Bi1-Cl1 = 2.545(3), Bi2-Cl2 = 2.546(3), Bi1-P1 = 2.745(3), Bi2-P2 = 2.726(3), Bi1-O1 = 2.701(7), Bi1-O2 = 2.657(7), Bi1-C1 = 2.250(1), Bi2-C2 = 2.253(1), Cl1-Bi1-O1 =

48.04(9), Cl1-Bi1-P1 = 80.99(9).

The compound **2** crystallizes in $P2_1/C$ space group containing the two cationic [L^{Ph}-BiCl] species with a bridging triflate anion, another triflate anion coordinates with the Bi1 center and a non-coordinating solvent molecule in the asymmetric unit (Fig.18, Table 2). Here in the molecular structure of compound **2**, the both Bi1-O1 and Bi2-O2 bond distances (2.701(7), 2.657(7) Å) are much less than the sum of their vanderwaal's radius (Σ_{rvdW}(Bi-O) = 3.59 Å), indicating the significant interactions between the O and Bi center. When we were trying to remove the chlorine atom from the compound **2** ([L^{Ph}_2-BiCl]) by AgOTf to obtain Bi(III) cationic species coordinated by two acenaphthene moieties, we got the compound **2**. So, instead of AgOTf we tried the reaction with TMSOTf. One advantage of using TMSOTf is that the produced TMSCl in the reaction mixture is volatile and can be easily removed during solvent evaporation in vacuum. The reaction of [L^{Ph}_2-BiCl] (compound **1**) and TMSOTf in 1:1 molar ratio generates the compound **3**. The single crystals of the compound **3** were grown from THF/n-pentane solution as intense yellow colour within 2 days. The compound **3** was characterized by single crystal X-ray diffraction analysis and ^{1}H, ^{13}C, ^{19}F, ^{31}P NMR analysis.

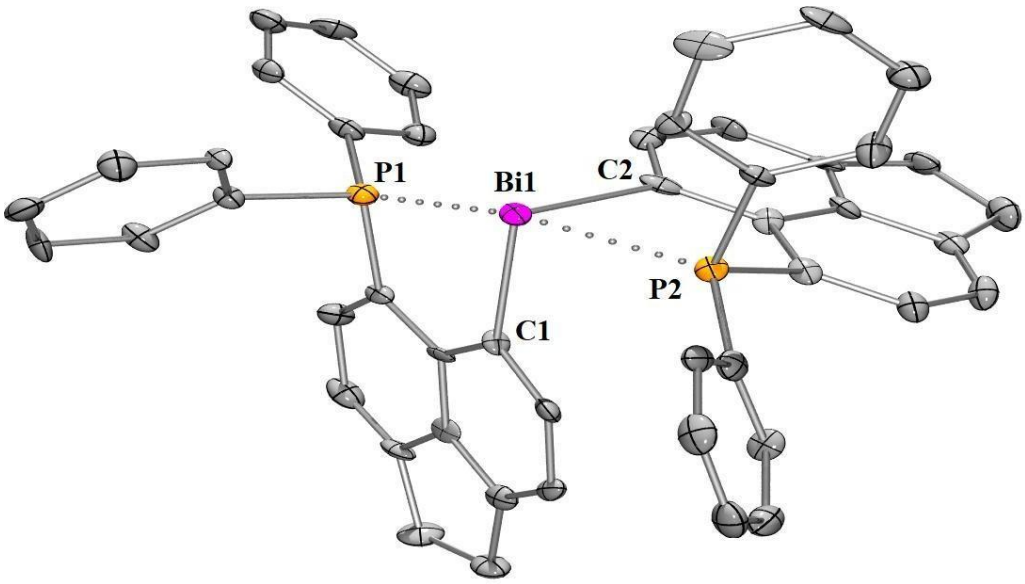

Fig. 19: Crystal structure of the Compound **3** (thermal ellipsoid at 30% probability, H atoms are excluded for clarity). The selected bond lengths [Å] and bond angles [°]:

Bi1-P1 = 2.890(4), Bi-P2 = 2.820(4), Bi1-C1 = 2.25(1), Bi1-C2 = 2.27(1),C1-Bi-C1 = 92.5(5).

The compound **3** crystallizes in P-1 space group (Fig 19, Table 3). Two triflate anion and four THF solvent molecules are present in the asymmetric unit. Here both the phosphorus center (P1, P2) are strongly coordinating to the Bi center, Whereas in the neutral compound i.e. compound **1** (**[L_2^{Ph} -BiCl]**) only one Phosphorus center was coordinating to the Bi center. This is obvious that the lewis acidity increses significantly in compound **3**. So the donation of electron density occurs from the two phosphorus centers to stabilize the Bi(III) cationic compound. This observation also supports from the ^{1}H and ^{31}P NMR spectrum which exhibit a significant downfield shift than the corresponding Neutral compound **1** ([L_2^{Ph}-BiCl]).

As mentioned earlier this mono-cationic compound **3** is an extremely potent sigma acceptor[24,25,26] ligand which has high possibility to bind with transition metals. The complex can tune the electronics of the transition metal center and exhibits various catalytic behaviour.[33] To investigate the sigma acceptor nature of this cationic center, we have reacted the compound **3** with CuCl to obtain compound **4**. The attempts of growing single crystals of the compound **4** were unsuccessful. But when we are analyzing the 31P NMR spectrum there is a huge downfield shift from -21.91 ppm (compound **1**) to 40.32 ppm (compound **4**). From this comparison we can predict the formation of Cu complex, where the two phosphorus atoms are donating the electron density to the transition metal, leads to the generation of Cu-Bi dative bond. Efforts to grow single crystals of the compound **4** is ongoing.

Compound **5** was obtained by the reaction of 5-bromo,6-diisopropylphosphino acenaphthene (L^{ipr}-Br) (1 eq) with n-BuLi (1 eq) at -78^{o}C. The 5-bromo,6-diisopropylphosphino acenaphthene (L^{ipr}-Br) was synthesized by above mentioned procedure. After two hours, $BiCl_3$ (1 eq) was added to obtain the [L^{ipr}-$BiCl_2$] compound (**5**). The yellow coloured single crystals of the compound **5** were obtained from DCM solution. The compound was charecterized by single crystal X-ray diffraction analysis which confirms the formation of the compound **5**.

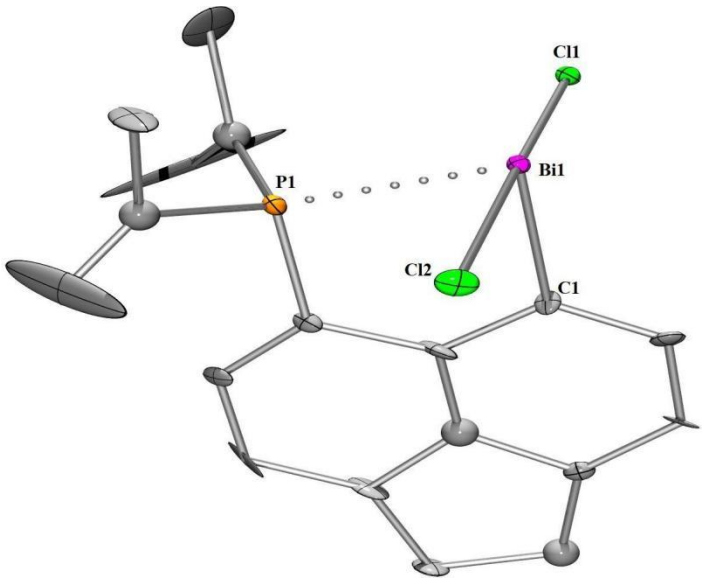

Fig. 20: Crystal structure of the compound **5** [L^{ipr}-$BiCl_2$] (thermal ellipsoid at 30% probability, H atoms are excluded for clarity). The selected bond lengths [Å] and bond angles [°]: Bi1-Cl= 12.678(5), Bi1-Cl2= 2.748(4), Bi-P1 = 2.713(5) , C1-Bi1-C1 = 87.8°(4), Cl1-Bi-Cl2 = 173.6°(1).

The similar compound [L^{Ph}-$BiCl_2$] (L^{Ph}=6-diphenylphosphinoacenaphth-5-yl) is reported from jens beckmann group.[31] Killian *et al* in 2020 reported the compound [L^{ipr}-$BiCl_2$] (3) as thermally unstable , not isolated.[28] But here we have successfully synthesized and characterized the compound. The compound **5** crystallizes in monoclinic $P2_1/c$ space group adopting the T-shaped geometry, where the Cl1-Bi-Cl2 angle is almost linear (Fig 20, Table 4). It is known that FLPs with long *peri* distances between E and P mainly shows repulsive interactions between E and P[29,30] but here the Bi1-P1 bond length is 2.713(5) Å which falls within the sum of the vanderwaal's radius (Σ_{rvdW}(Bi-P) = 3.87 Å) indicating there is an attractive interactions between the Bi and the P center.

Our main goal was to make the cationic complex of this compound to increase the lewis acidity at the Bismuth centre.The interaction between the phosphorus atom at the 6th position of the acenaphthene and Bismuth atom at the 5th position of the acenaphthene was also the centre of interest.To obtain the cationic species of the compound **6**, **[L^{ipr}-$BiCl_2$]** and AgOTf were combined in 1:1 molar ratio in DCM solution. The resulted compound **6** was obtained as colourless crystal in DCM/ n-pentane solution. The crystals of the compound **6** were characterized by single crystal X-ray diffraction analysis which confirms the formation of the product **6**.

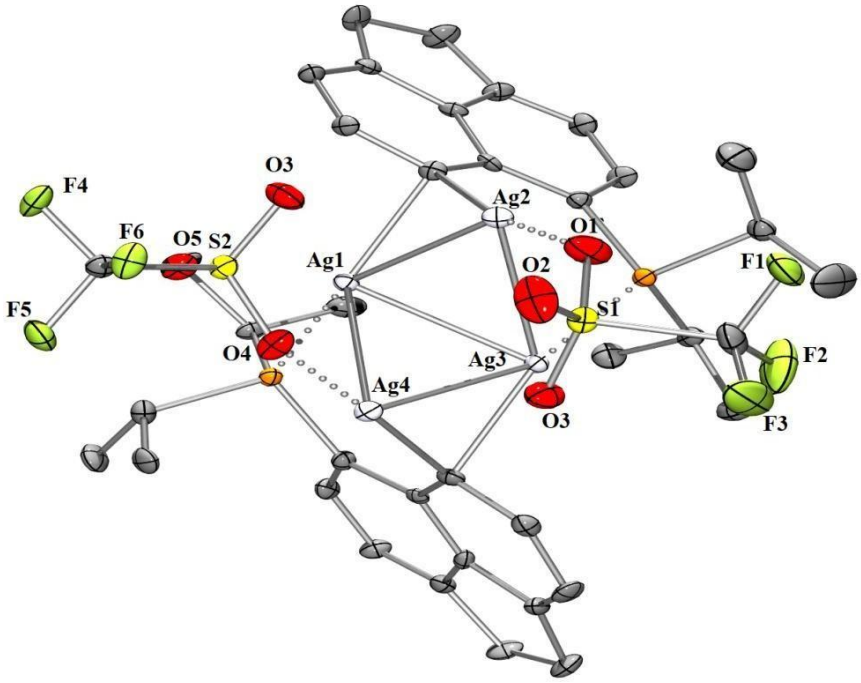

Fig. 21: Crystal structure of the Compound **6** (thermal ellipsoid at 30% probability, H atoms and non-coordinating solvent molecules are excluded for clarity). The selected bond lengths [Å] and bond angles [°]: Ag1-Ag2 = 2.842(8), Ag1-Ag4 = 2.927(8), Ag2-Ag3 = 2.897(9), Ag3-Ag4 = 2.766(9), O4-Ag4 = 2.187(4), Ag1-Ag4-Ag3 = 60.22(2), Ag1-Ag3-Ag2 = 59.16(2).

The compound **6** crystallizes in monoclinic $P2_1/n$ space group cointaining two weakly coordinating triflate anion and two non-coordinating solvent molecule in the asymmetric unit (Fig. 21, Table 5). In the molecular structure of the compound 5 the all Ag-Ag distances (2.927(8) - 2.187(4)) are much less than the sum of their vanderwaal's radius (Σ_{rvdW}(Ag-Ag) = 3.44 Å) and the compound adopts a bent geometry.

Then the reaction of L^{iPr}-Br and $BiCl_3$ in 3:1 molar ratio obtained the compound **7**; [L^{iPr}_3Bi] by following the literature procedure.[34] The compound **7** has been characterized by ^{31}P NMR analysis. The similar type of complex [L^{Ph}_3Ga] has been reported by Jens Beckmann *et al* where they synthesized the Ni/Pd coordinated gallium complex, consisting Ni/Pd→Ga dative bond.[36] Almost all the reported Z-type

ligands of group 13,14 or even group 15 contains the ligand framework diorganophosphino groups in ortho position of the phenyl group.[35,36] So we have synthesized the *peri*-substituted 6-diisopropylphosphino-acenaphth-5-yl compound **7**.

Furthermore we investigated the reactivity of the compound **7** with $Ni(COD)_2$, CuCl, $PdCl_2$ to observe the potential of the compound to bind with the transition metals, acting as a Z-type ligand. In all the cases, the reactions leads to the formation of the compound **5** i.e. [L^{iPr}-$BiCl_2$] which is highly stable. We are still attempting to grow perfect single crystals of these compounds despite this disadvantage.

Conclusion:

In this study, we have successfully synthesized L^{iPr}-Br and L^{Ph}-Br which are the precursors of 6-diphenylphosphinoacenaphth-5-yl-(**L^{Ph}**) and 6-diisopropylphosphinoacenaphth-5-yl-(**L^{iPr}**) ligands. we have successfully synthesized **$[L^{Ph}_2BiCl]$** (**1**) and isolation of **$[L^{Ph}_2Bi^+](OTf^-)$ (3)** was achieved and when we add 1 equivalent TMSOTf with compound **1.** But, adding 1 equivalent AgOTf with **$[L^{Ph}_2BiCl]$** (**1**) we got **$[L^{Ph}BiCl^+](OTf^-)$ (2).** Then the reaction of **$[L^{Ph}_2Bi^+](OTf^-)$** with CuCl in 1:1 molar ratio yielded the complex **4,** which has charecterized by ^{31}P NMR analysis. After that the reaction of Compound L^{iPr}-Br with $BiCl_3$ produced [L^{ipr}-$BiCl_2$]; compound **5**. When we are trying to abstract one of the chlorine atom from this compound **5** by adding 1 eq. AgOTf, we got the Ag-Cluster (**6**). The resulting molecules are characterized using nuclear magnetic resonance (NMR) spectroscopy and single-crystal X-ray diffraction (SC-XRD) analysis. We also have successfully synthesized the compound **7**. The detailed reactivity studies of the Compound **7** are currently underway which is highly likely to exhibit metal coordination leads to catalytic activity at the metal center as stated earlier. Overall, the resulting structures will provide valuable insights into the potential catalytic behavior of these species and offer potential avenues for small molecule activation, which can be analyzed in detail by further studies.

References

1) J. Heine, B. Peerless, S. Dehnen, C. Lichtenberg, *Angew. Chem. Int. Ed*. **2023**, *62*, e202218771.

2) W. Baumann, A. Schulz, A. Villinger, *Angew. Chem. Int. Ed*. **2008**, *47*, 9530 – 9532.

3) H. Haldar, Cem. B. Yildiz, M. Majumdar, *ChemPlusChem,* **2023**, *88*, e202300211.

4) C. Lichtenberg, *Chem. Commun*., **2021**, *57*, 4483–4495.

5) J. Ramler, K. Hofmann, C. Lichtenberg, *Inorg. Chem*. **2020**, *59*, 3367−3376.

6) R. J. Schwamm, B. M. Day, M. P. Coles, C. M. Fitchett, *Inorg. Chem*. **2014**, *53*, 3778−3787.

7) J. Ramler, C. Lichtenberg, *Chem. Eur. J*. **2020**, *26*, 10250 – 10258.

8) M. Olaru, D. Duvinage, E. Lork, S. Mebs, J. Beckmann, *Angew. Chem. Int. Ed.* **2018**, *57*, 10080 –10084.

9) J. Bresien, A. Schulz, M. Thomas, A. Villinger, *Eur. J. Inorg. Chem*. **2019**, 1279–1287.

10) T. A. Engesser, M. R. Lichtenthaler, M. Schleep, Ingo Krossing, *Chem. Soc. Rev.*, **2016**, *45*, 789--899.

11) A. F. Hill, G. R. Owen, A. J. P. White, D. J. Williams, *Angew. Chem. Int. Ed.* **1999**, *38*, No. 18.

12) M. Sircoglou, S. Bontemps, M. Mercy, N. Saffon, M. Takahashi, G. Bouhadir, L. Maron, D. Bourissou, *Angew. Chem. Int. Ed*. **2007**, *46*, 8583 –8586.

13) P. Gualco, T.P. Lin, M. Sircoglou, M. Mercy, S. Ladeira, G. Bouhadir, L.M. Perez, A. Amgoune, L. Maron, F.P. Gabbai, D.Bourissou, *Angew. Chem*. **2009**, *121*, 10076-10079.

14) H. Kameo, T. Kawamoto, S. Sakaki, H. Nakazawa, *Organometallics*. **2014**, *33*, 5960- 5963.

15) H. Kameo, D. Bourissou, S. Sakaki, H. Nakazawa, *Organometallics*. **2014**, *33*, 6557- 6567.

16) H. Kameo, T. Kawamoto, S. Sakaki, D. Bourissou, H. Nakazawa, *Chem. Eur. J*. **2016**, *22*, 2370-2375.

17) H. Kameo, K. Ikeda, H. Nakazawa, S. Takemoto, H. Matsuzaka, *Dalton Trans*. **2016**, *45*, 7570-7580.

18) H. Yang, F. P. Gabbaï, *J. Am. Chem. Soc*. **2015**, *137*, 13425−13432.

19) D. You, F. P. Gabbaï, *J. Am. Chem. Soc*. **2017**, 1*39*, 6843−6846.

20) D. You, H. Yang, S. Sen, F. P. Gabbaï, *J. Am. Chem. Soc*. **2018**, *140*, 9644−9651.

21) Y. H. Lo, F. P. Gabbaï, *Angew. Chem. Int. Ed*. **2019**, *58*, 10194–10197.

22) C. R. Wade, F. P. Gabbaï, *Angew. Chem. Int. Ed*. **2011**, *50*, 7369 –7372

23) E. Wächtler, R. Gericke, T. Block, R. Pöttgen, J. Wagler*, Inorg. Chem.* **2020**, *59*, 20, 15541–15552.

24) T. Lin, L. Ke, F. P. Gabbaï, *Angew. Chem. Int. Ed*. **2012**, *51*, 4985 –4988

25) P. Coburger, A. G. Buzanich, F. Emmerling, J. Abbenseth, *Chem. Sci.*, 2024.

26) C. Tschersich, C. Limberg, S. Roggan, C. Herwig, N. Ernsting,S. Kovalenko, S. Mebs, *Angew. Chem. Int. Ed*. **2012**, *51*, 4989 –4992.

27) J. Beckmann, T. G. Do, S. Grabowsky, E. Hupf, E. Lork, S. Mebs, *Z. Anorg. Allg. Chem.* **2013**, 2233–2249.

28) P. Wawrzyniak, A. L. Fuller, A. M. Z. Slawin, P. Kilian. *Inorg. Chem.* **2009**, *48,* 2500–250.

29) P. S. Nejman, T. E. Curzon, M. Buhl, D. McKay, J. D. Woollins, S. E. Ashbrook, D. B. Cordes, A. M. Z. Slawin, P. Kilian, *Inorg. Chem*. **2020**, *59*, 5616−5625.

30) A. Tsurusaki, T. Sasamori, A. Wakamiya, S. Yamaguchi, K. Nagura, S. Irle, N. Tokitoh, *Angew. Chem. Int. Ed.* **2011**, *50*, 10940 –10943.

31) A. Tsurusaki, T. Sasamori, N. Tokitoh, *Chem. Eur. J*. **2014**, *20*, 3752 – 3758.

32) E. Hupf, E. Lork, S. Mebs, L. Chęcinska, J. Beckmann, *Organometallics* **2014**, *33*, 7247−7259.

33) L. C. Wilkins, Y. Kim, E. D. Litle, F. P. Gabbaï, *Angew. Chem. Int. Ed*. **2019**, *58*, 18266 –18270.

34) A. Hermannsdorfer, M. Driess, *Angew. Chem. Int. Ed.* **2020**, *59*, 23132–23136

35) B. A. Chalmers, C. B. E. Meigh, P. S. Nejman, M. Buhl, T. Lebl, J. D. Woollins, A. M. Z. Slawin, P. Kilian, *Inorg. Chem*. **2016**, *55*, 7117−7125

36) S. Furan, M. Molkenthin, K. Winkels, E. Lork, S. Mebs, E. Hupf, J. Beckmann, *Organometallics* **2021**, *40*, 3785−3796

37) M. A. Bennett, S. K. Bhargava, N. Mirzadeh, S.H. Privér, *Coord. Chem. Rev*. **2018**, *370*, 69−128.

38) C. J. Carmalt, L. J. Farrugiab, N. C. Norman, *J. Chem. SOC., Dalton Trans.,* **1996**, 443-454.

Appendix

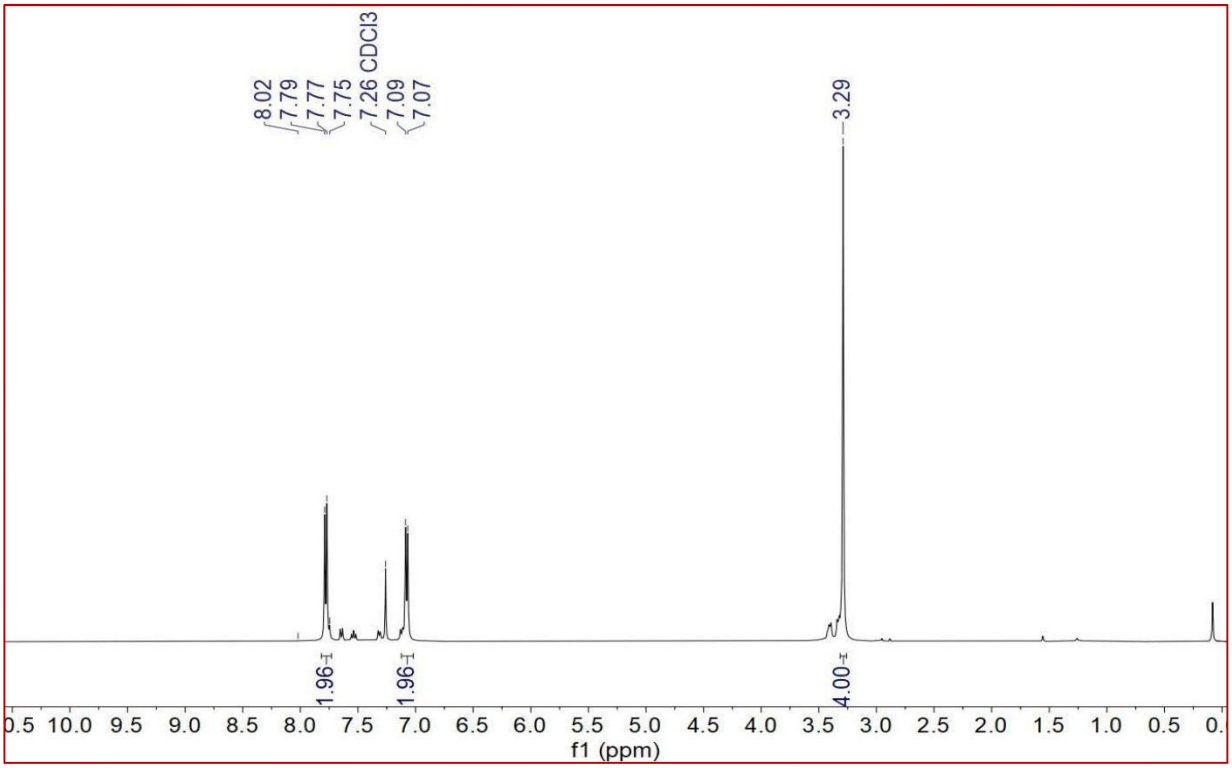

Fig. 22: ^{1}H NMR spectrum (400 MHz, in CDCl3, 298K) of compound 5,6-dibromoacenaphthene.

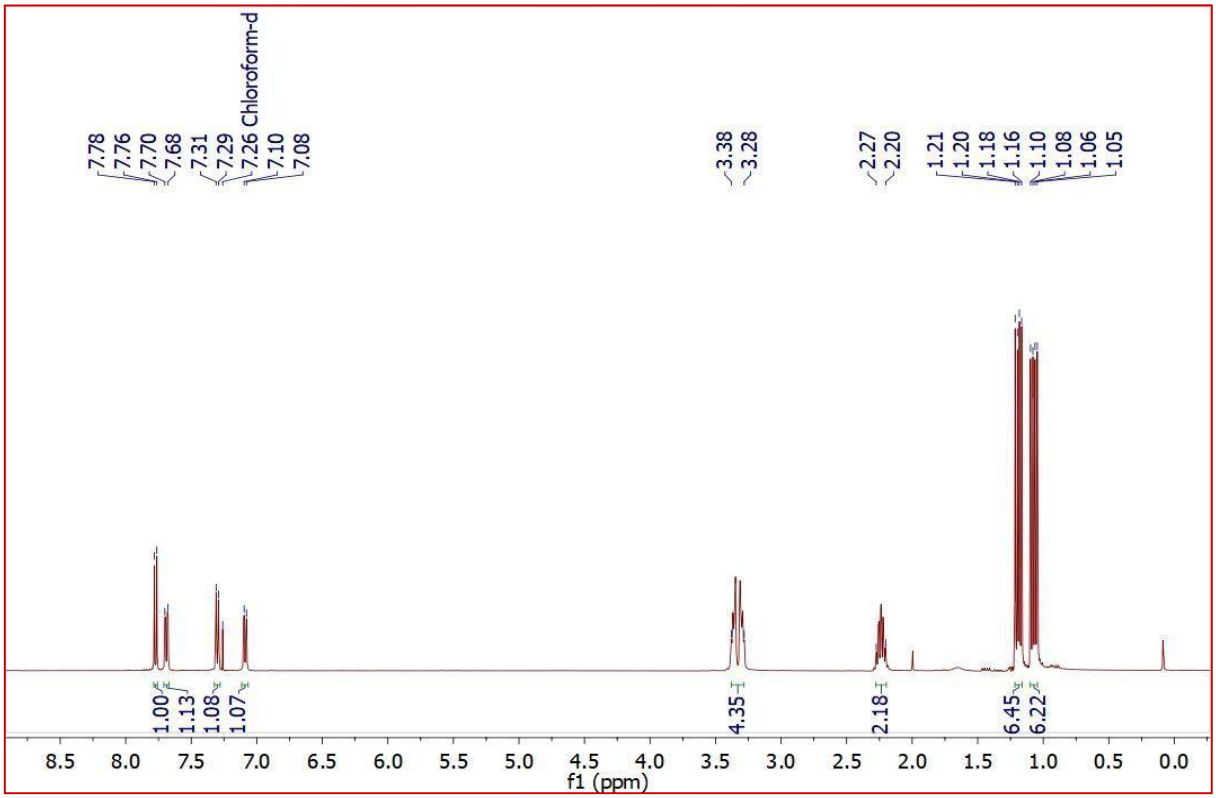

Fig. 23: ^{1}H NMR spectrum (400 MHz, in CDCl3, 298K) of compound **L^{iPr}-Br**.

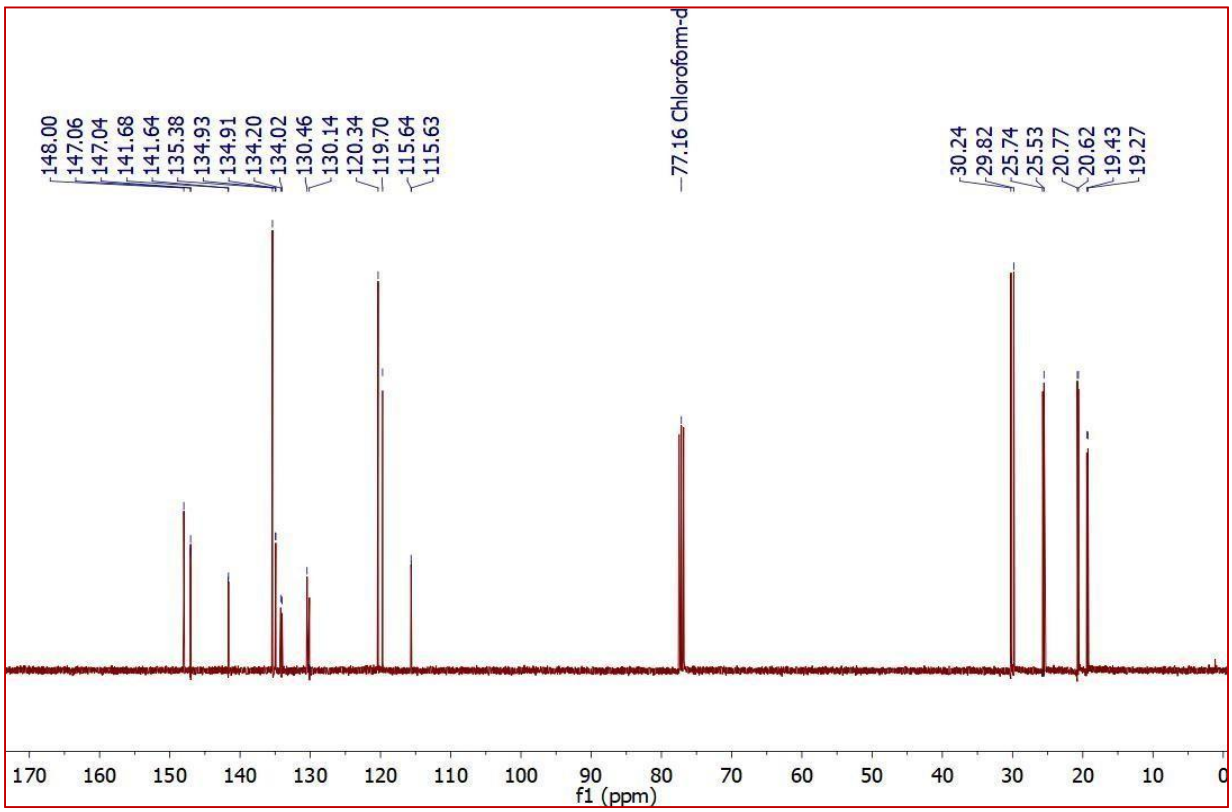

Fig. 24: $^{13}C\{^{1}H\}$ NMR spectrum (400 MHz, in CDCl3, 298K) of compound **L^{iPr}-Br**.

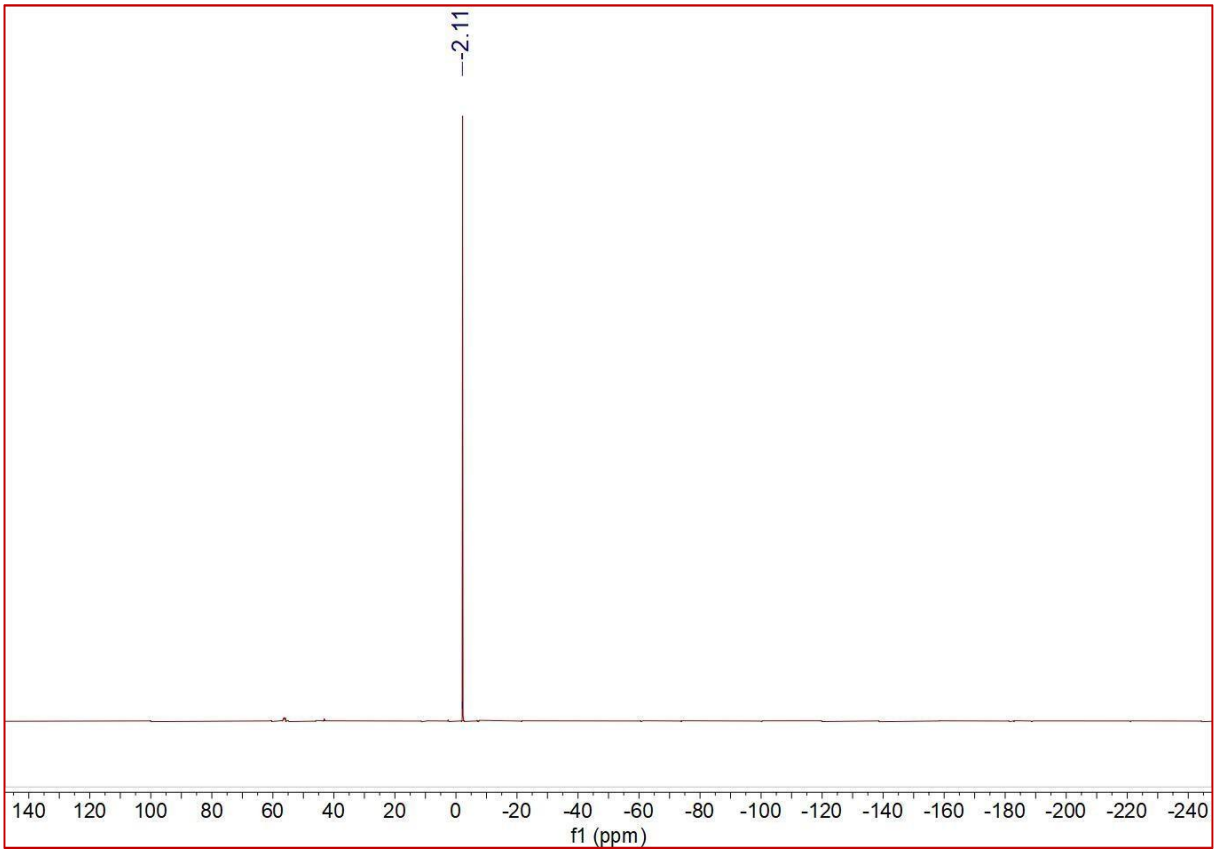

Fig. 25: $^{31}P\{^{1}H\}$ NMR spectrum (400 MHz, in CDCl3, 298K) of compound **L^{iPr}-Br**.

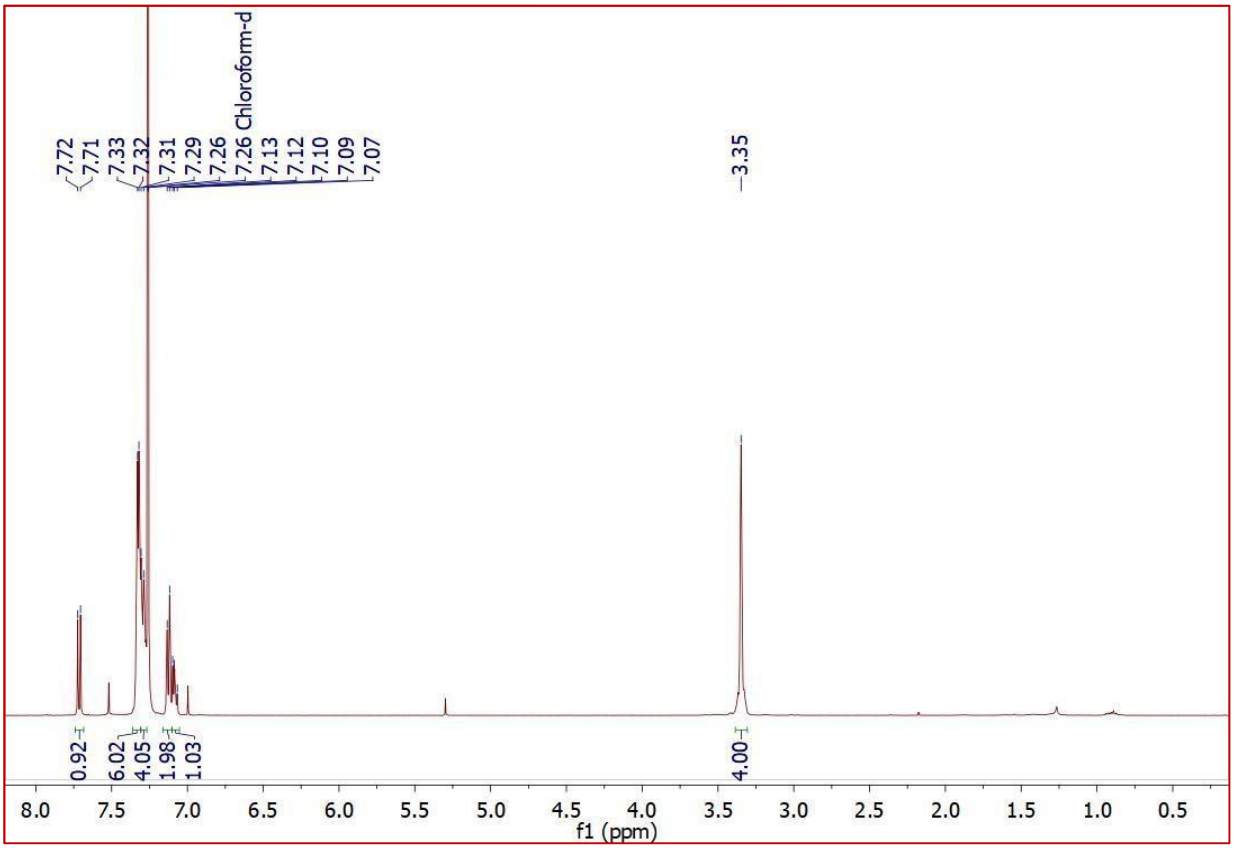

Fig. 26: ^{1}H NMR spectrum (400 MHz, in CDCl3, 298K) of compound **L^{Ph}-Br**.

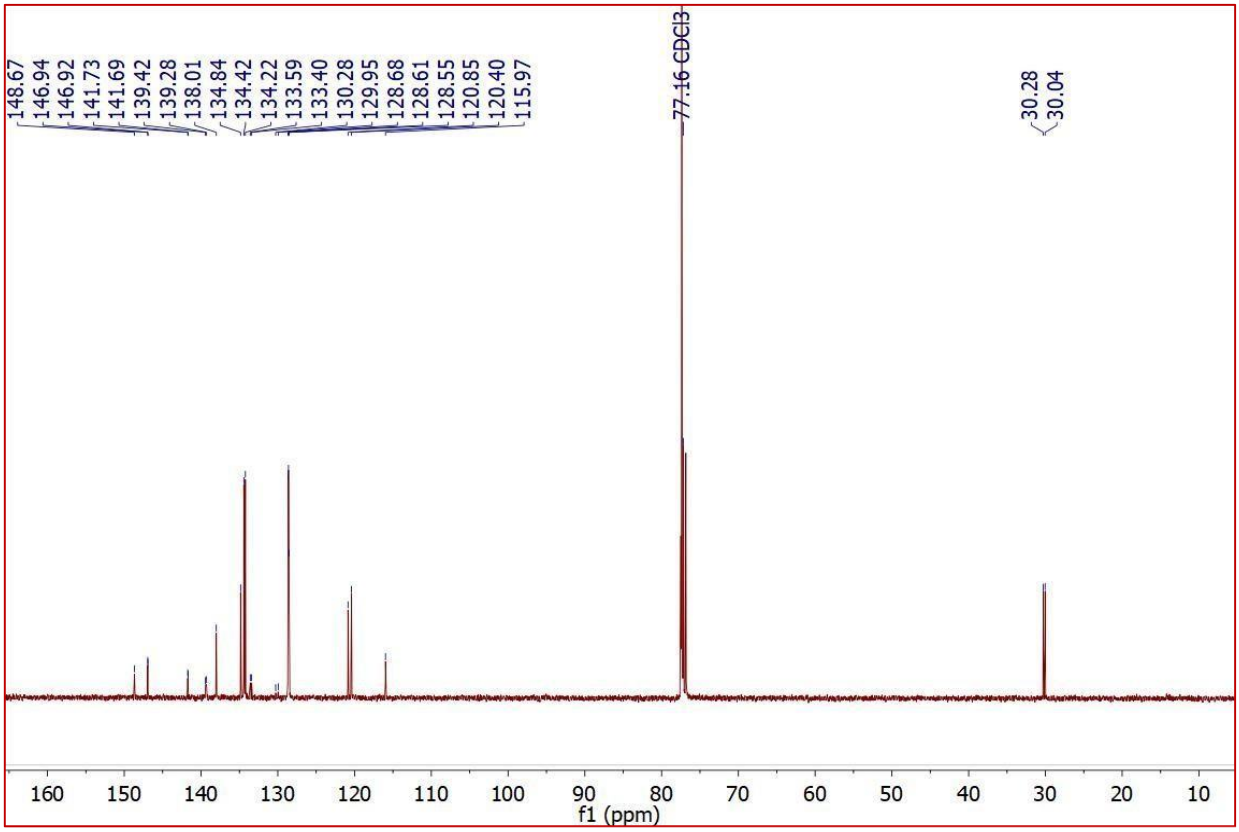

Fig. 27: ^{13}C{^{1}H} NMR spectrum (400 MHz, in CDCl3, 298K) of compound **L^{Ph}-Br**.

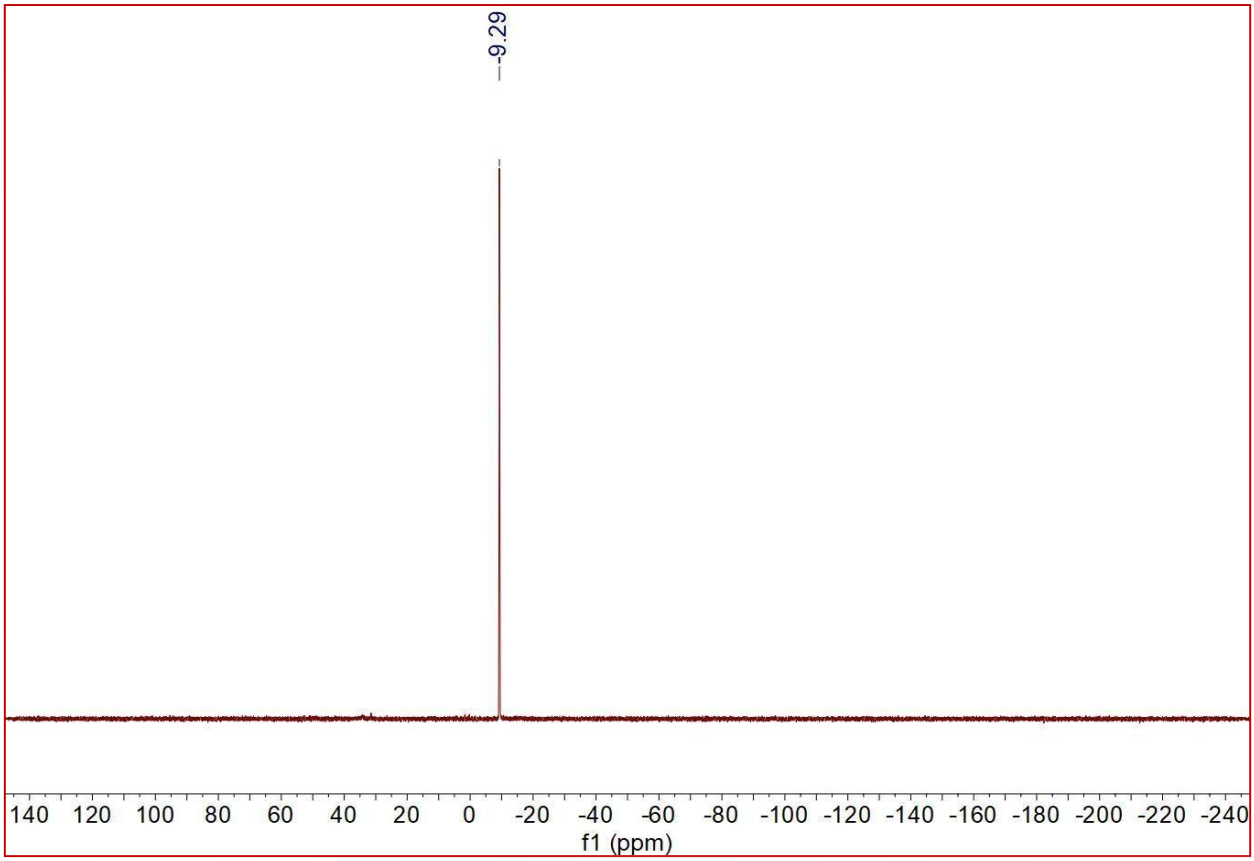

Fig. 28: $^{31}P\{^{1}H\}$ NMR spectrum (400 MHz, in CDCl3, 298K) of compound **L^{Ph}-Br**.

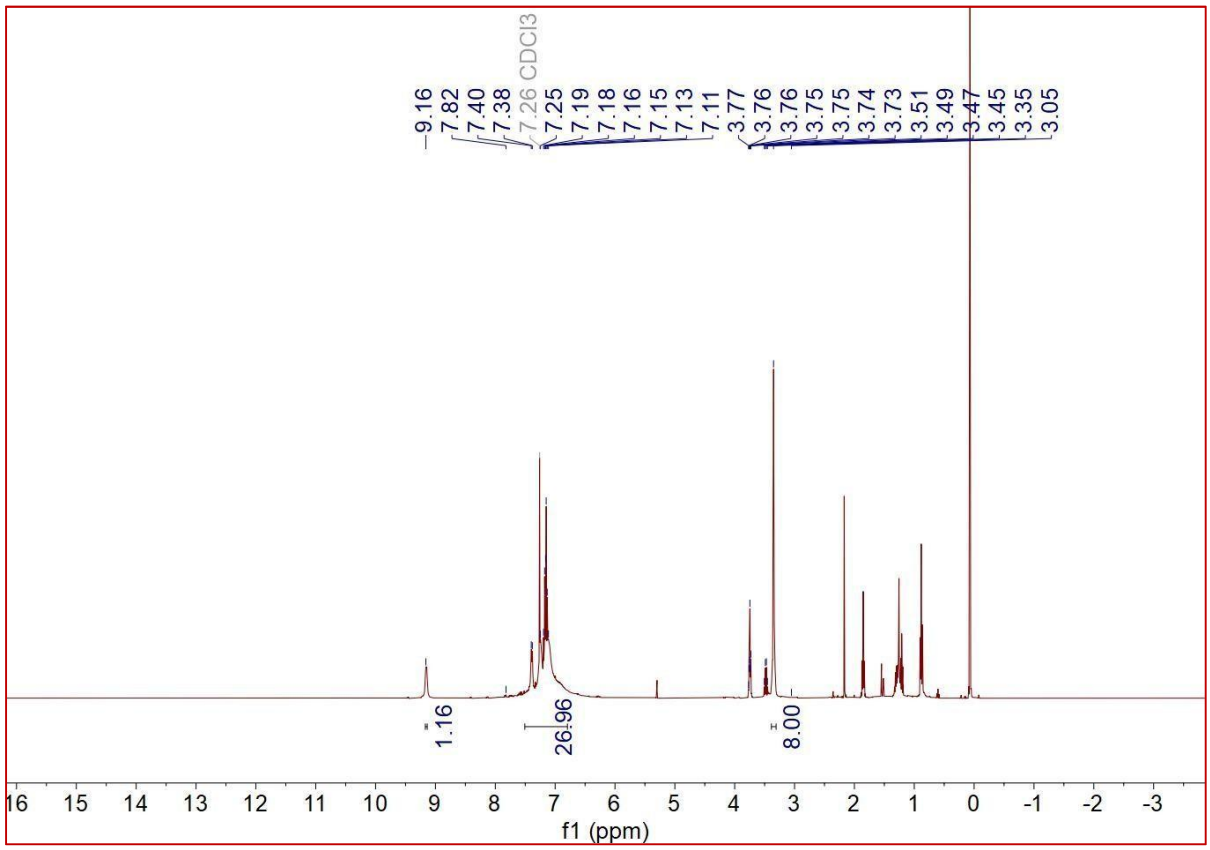

Fig. 29: ^{1}H NMR spectrum (400 MHz, in CDCl3, 298K) of compound **1**.

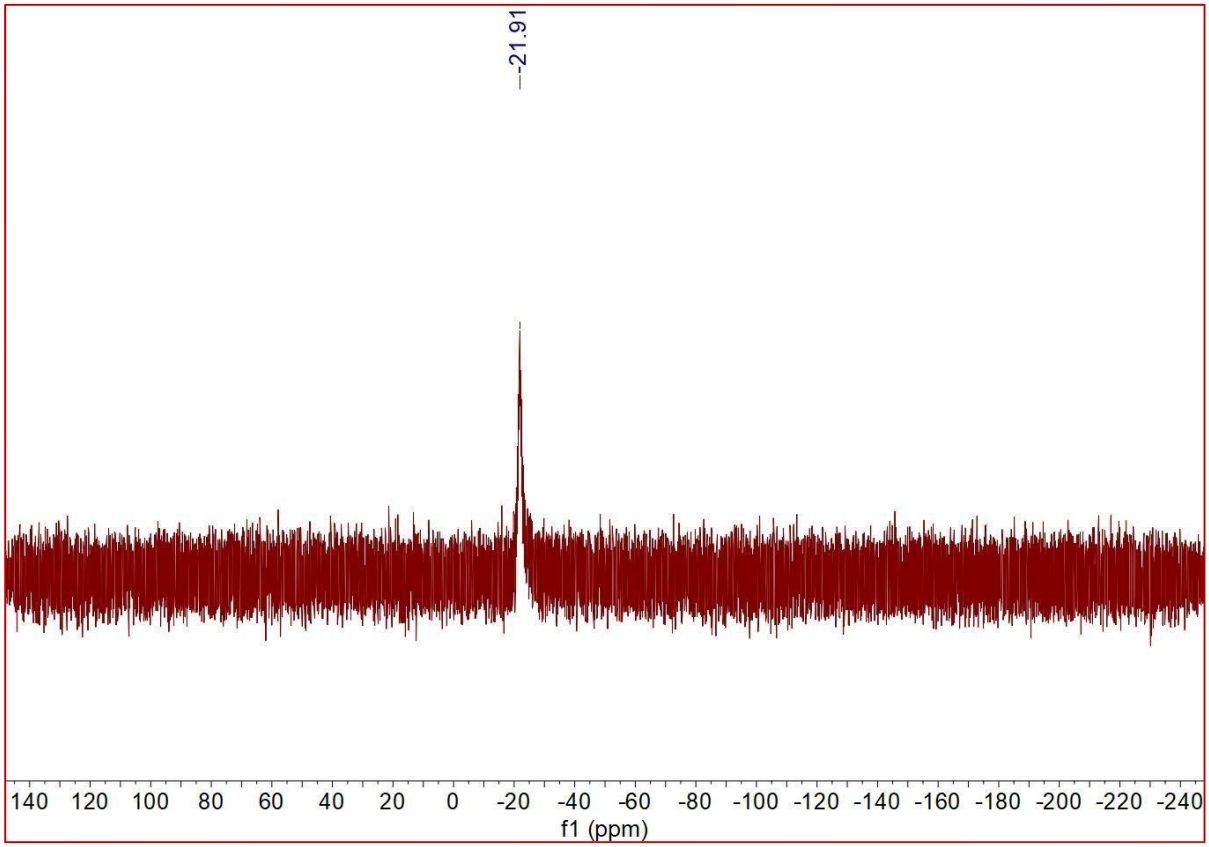

Fig. 30: ^{31}P{^{1}H} NMR spectrum (400 MHz, in CDCl3, 298K) of compound **1**.

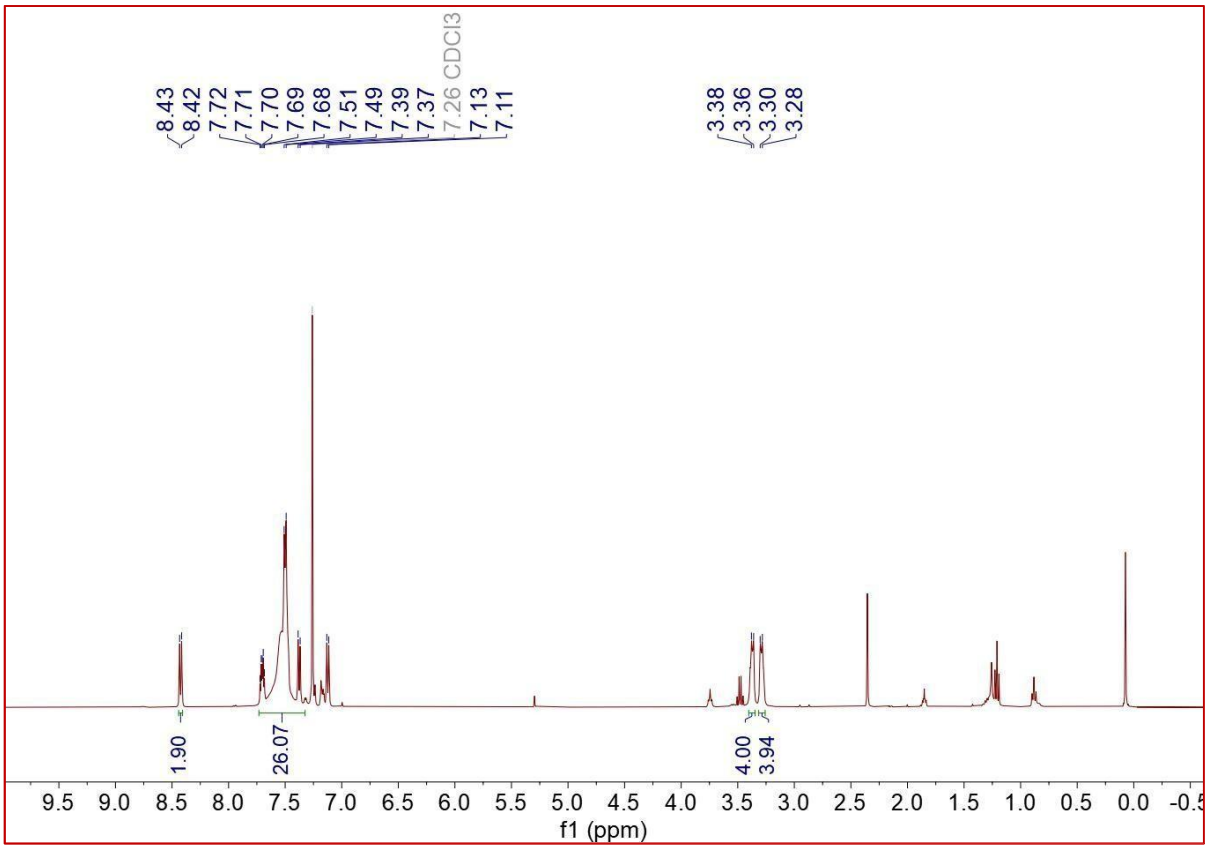

Fig. 31: ^{1}H NMR spectrum (400 MHz, in CDCl3, 298K) of compound **3**.

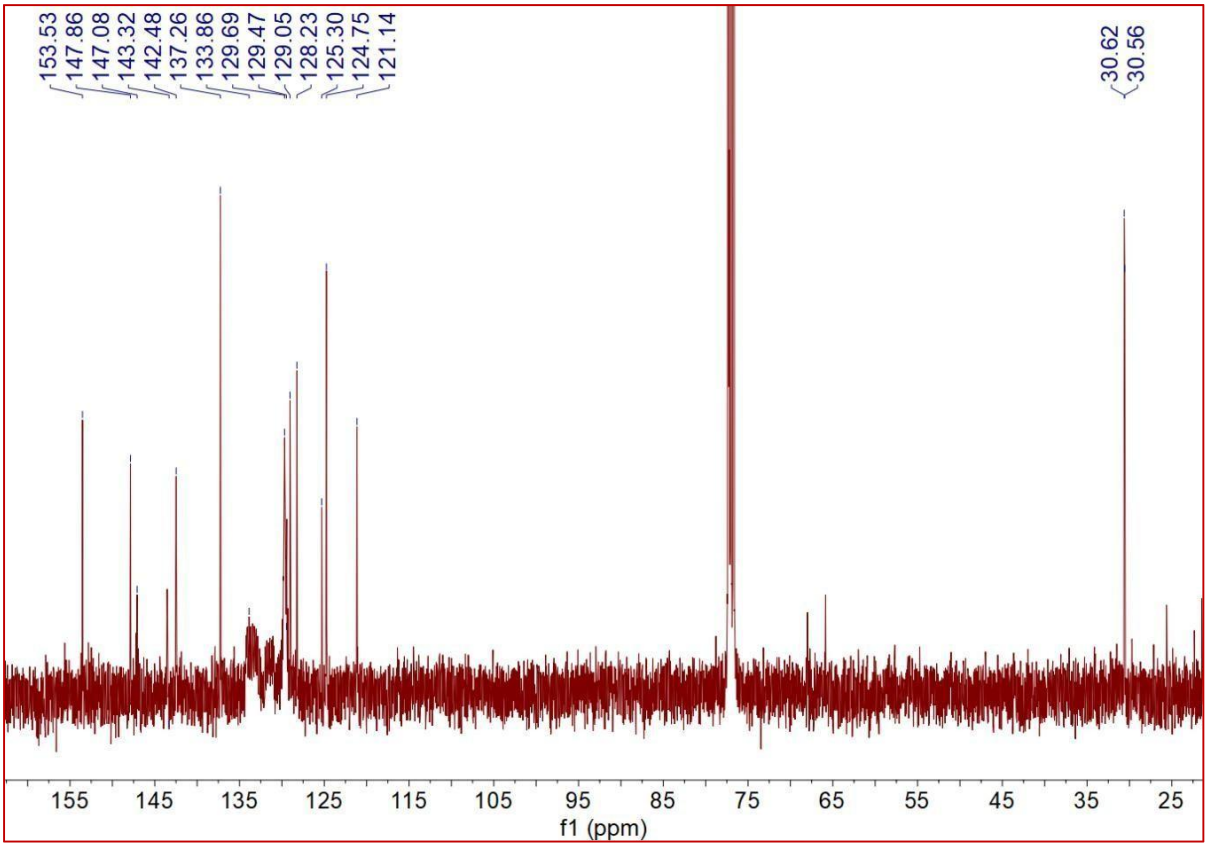

Fig. 32: ^{13}C{^{1}H} NMR spectrum (400 MHz, in CDCl3, 298K) of compound **3**.

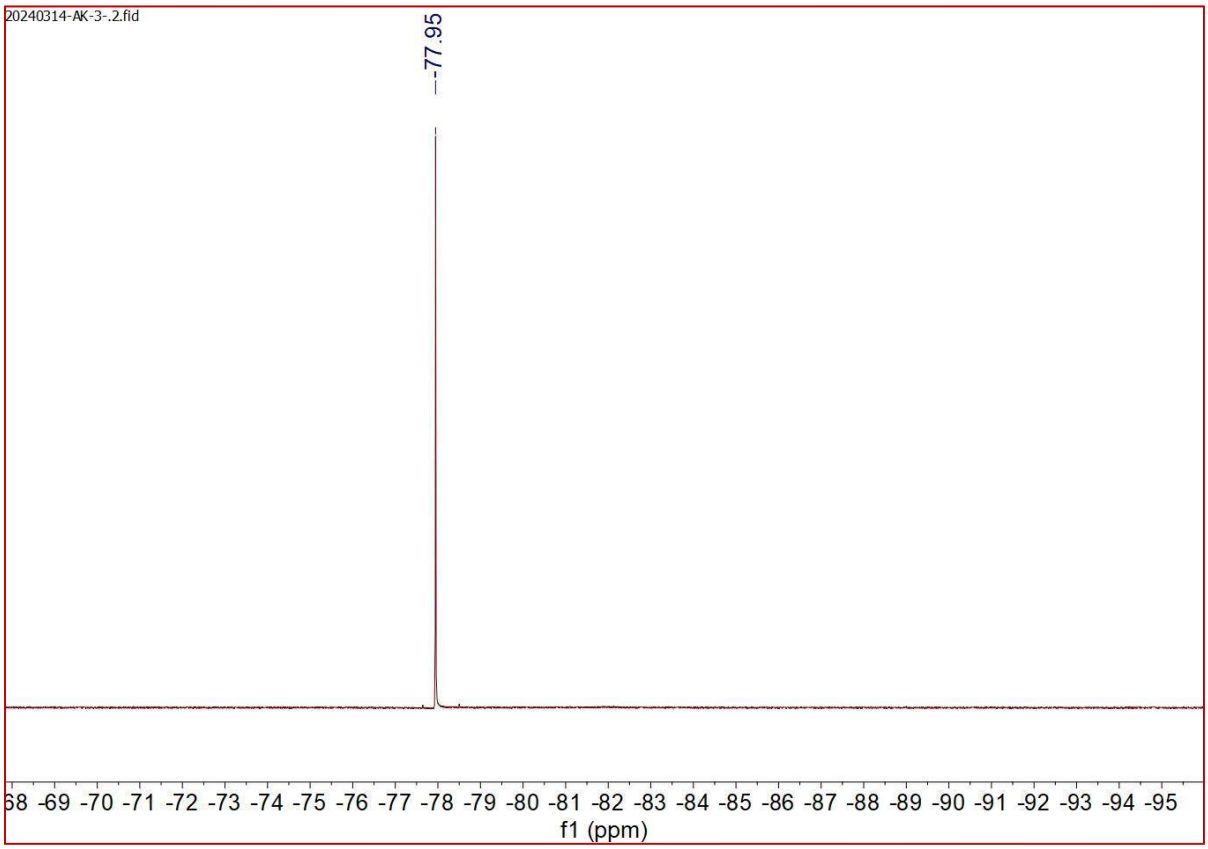

Fig. 33: $^{19}F\{1H\}$ NMR spectrum (400 MHz, in CDCl3, 298K) of compound **3**.

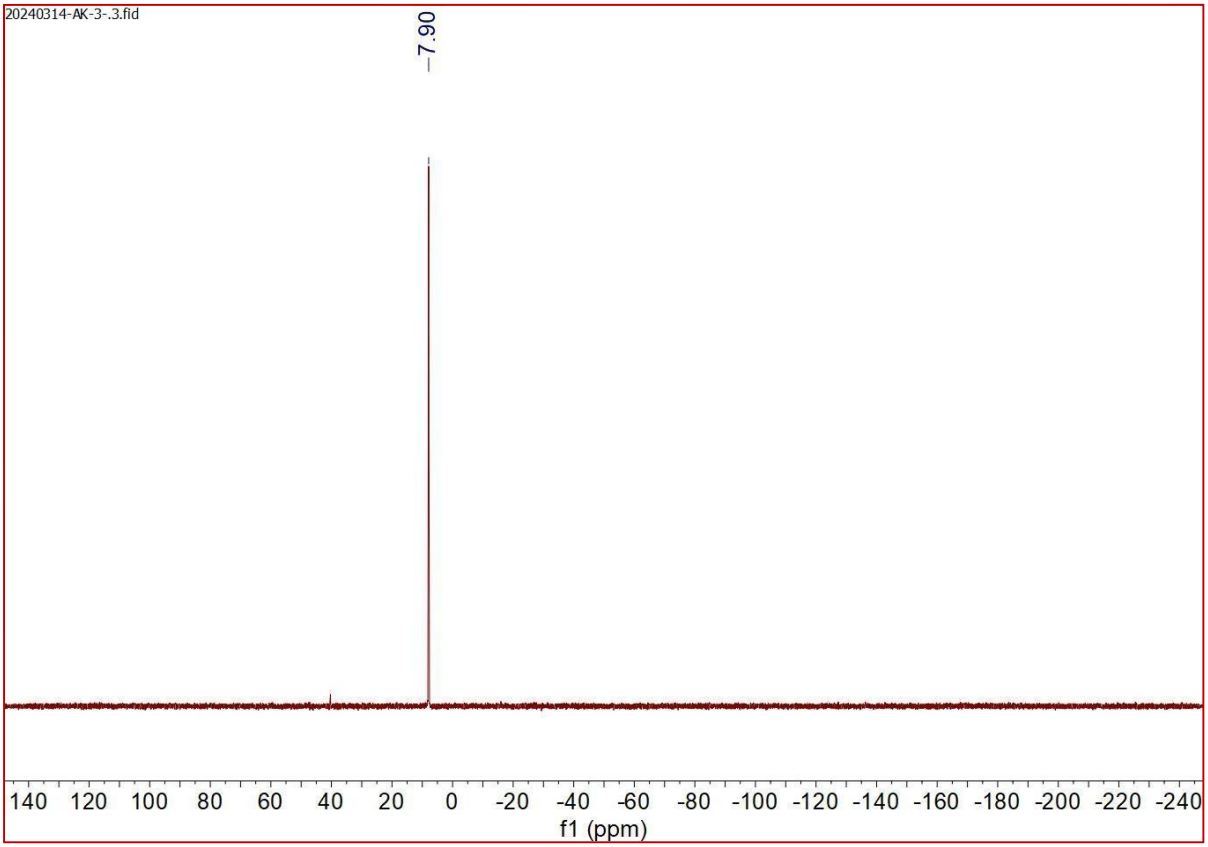

Fig. 36: $^{31}P\{^{1}H\}$ NMR spectrum (400 MHz, in CDCl3, 298K) of compound **7**.

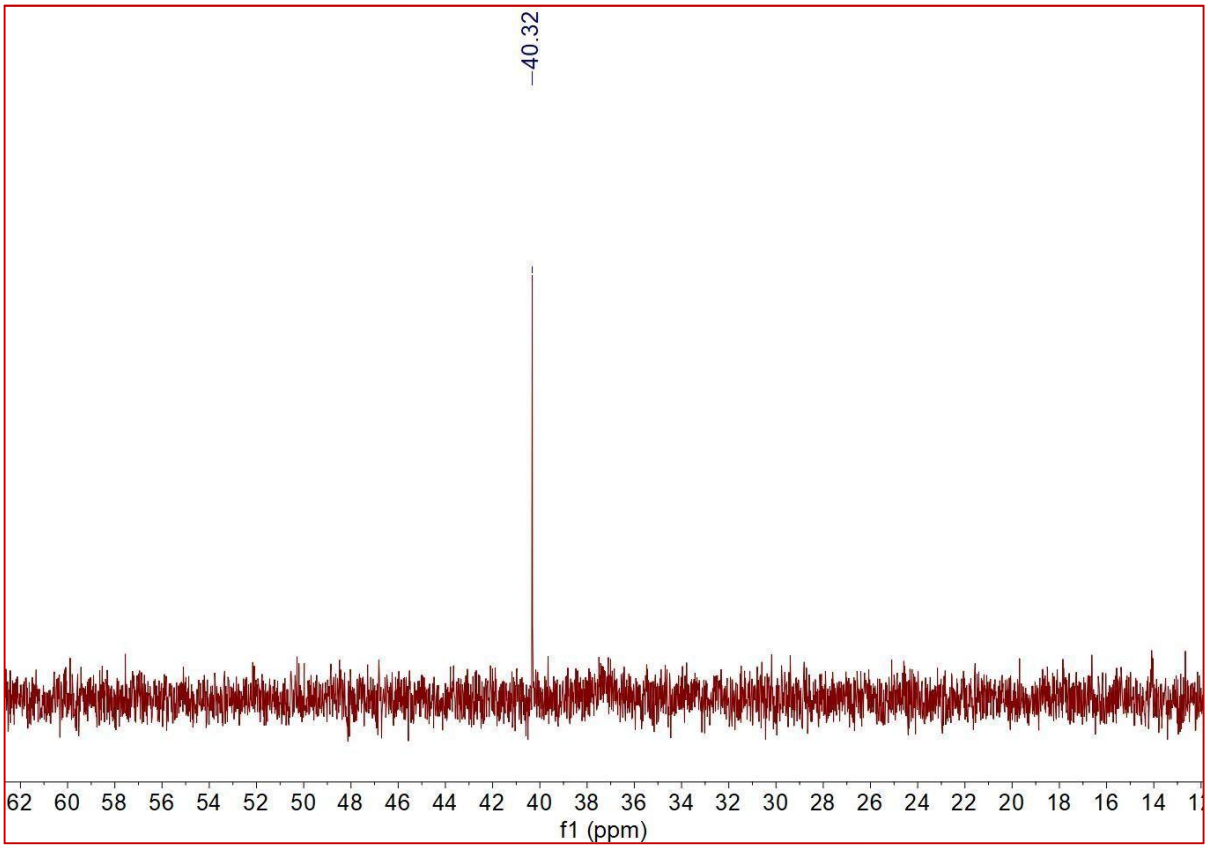

Fig. 35: $^{31}P\{^{1}H\}$ NMR spectrum (400 MHz, in CDCl3, 298K) of compound **4**.

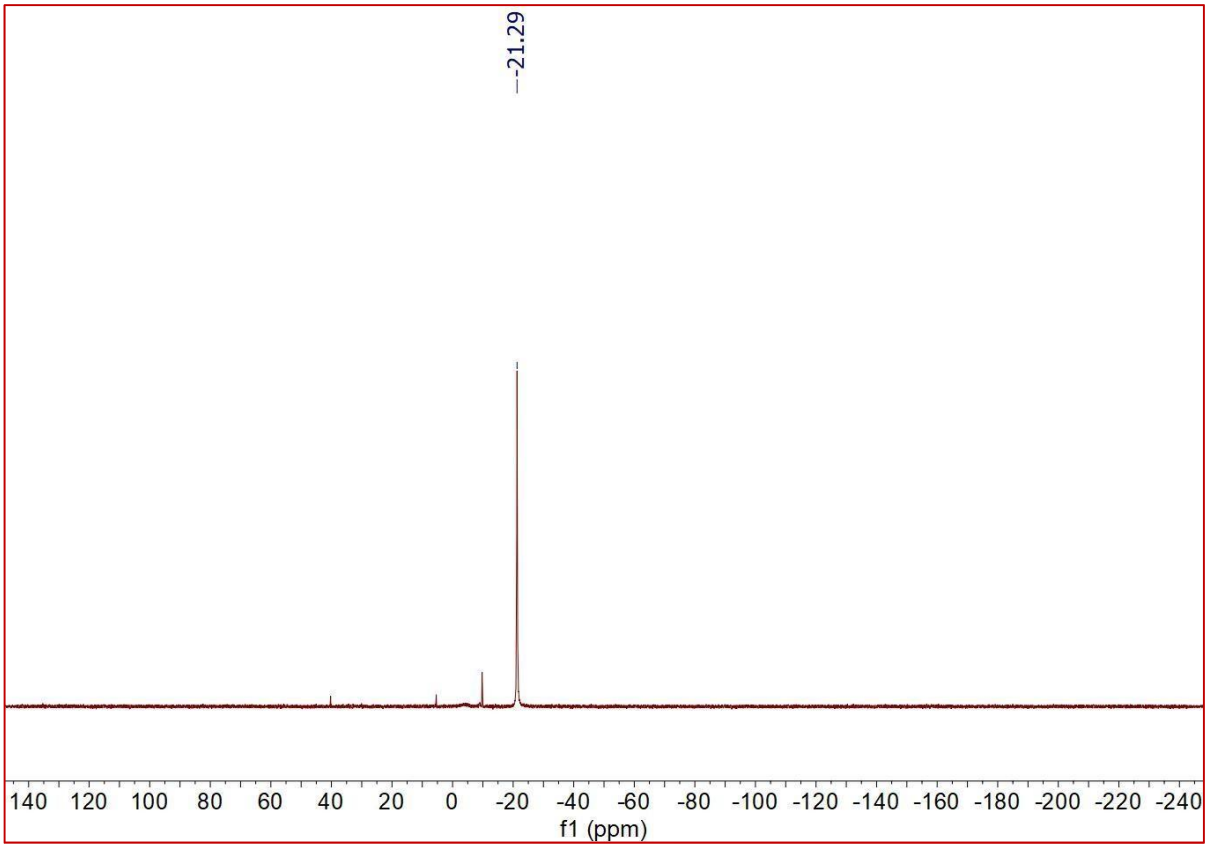

Fig. 36: $^{31}P\{^{1}H\}$ NMR spectrum (400 MHz, in CDCl3, 298K) of compound **7**.

Table 1: Crystal data and structure refinement for compound **1**

Empirical formula	$CHBiClPF_{0.05}Br_{0.05}$	
Formula weight	293.13	
Temperature/K	296.15	
Wavelength	0.71073 Å	
Crystal system	triclinic	
Space group	P-1	
Unit cell dimensions	a = 11.0358(16)Å	α = 73.777(4)°
	b = 12.8005(18)Å	β = 82.235(4)°
	c = 17637(3) Å	γ = 85.303(4)°
Volume	2367.7(6)	
Z	21	
Density(calculated)	4.317	
Absorption coefficient	40.247	
F(000)	2606.0	
Theta range for data collection	4.202 to 50.1	
Index ranges	-13<= h <=13, -15<= k <=15, -21<= l <= 21	
Reflections collected	67620	
Independent reflections	8368	
Completeness to theta	99.99%	
Absorption correction	multi-scan	
Max. and Min. Transmission	0.7452 and 0.4235	
Refinement method	Full-matrix least-squares on F^2	
Data/ restraints/ parameters	8368/0/550	
Goodness-of-fit on F^2	1.300	
Final R indices [I>2 sigma(I)]	R1 = 0.0412, wR2 = 0.1429	
R indices (all data)	R1 = 0.0444, wR2 = 0.1463	
Largest diff. peak and hole	5.532 and -1.594 e.$Å^{-3}$	

Table 2: Crystal data and structure refinement for compound **2**

Empirical formula	$C_{41}H_{41}B_{41}Cl_{41}I_{41}P_{41}SbBiOSF$	
Formula weight	9301.942	
Temperature/K	273.15	
Wavelength	0.71073 Å	
Crystal system	monoclinic	
Space group	$P2_1/c$	
Unit cell dimensions	a = 9.127(3)Å	α = 90°
	b = 25.433(9)Å	β = 90.037°
	c = 21.822(7) Å	γ = 90°
Volume	5066(3)	
Z	1	
Density(calculated)	3.049	
Absorption coefficient	8.159	
F(000)	4135.3	
Theta range for data collection	2.46 to 53.78	
Index ranges	-11<= h <=11, -32<= k <=32, -27<= l <= 27	
Reflections collected	45500	
Independent reflections	10813	
Completeness to theta	99.85%	
Absorption correction	multi-scan	
Max. and Min. Transmission	0.7454 and 0.5049	
Refinement method	Full-matrix least-squares on F^2	
Data/ restraints/ parameters	10813/0/659	
Goodness-of-fit on F^2	0.953	
Final R indices [I>2 sigma(I)]	R1 = 0.0547, wR2 = 0.1151	
R indices (all data)	R1 = 0.1063, wR2 = 0.1511	
Largest diff. peak and hole	2.72 and -2.43 e.Å^{-3}	

Table 3: Crystal data and structure refinement for compound **3**

Empirical formula	CHBiFOPS	
Formula weight	320.03	
Temperature/K	273.15	
Wavelength	0.71073 Å	
Crystal system	triclinic	
Space group	P-1	
Unit cell dimensions	a = 14.093(6)Å	α = 90.088(10)°
	b = 17.819(8)Å	β = 100.495(10)°
	c = 19.752(8) Å	γ = 90.025(10)°
Volume	4877(4)	
Z	1	
Density(calculated)	0.109	
Absorption coefficient	0.919	
F(000)	138.0	
Theta range for data collection	2.096 to 47.15	
Index ranges	-15<= h <=15, -19<= k <=19, -22<= l <= 22	
Reflections collected	64077	
Independent reflections	14241	
Completeness to theta	97.90%	
Absorption correction	multi-scan	
Max. and Min. Transmission	0.7449 and 0.3931	
Refinement method	Full-matrix least-squares on F^2	
Data/ restraints/ parameters	14241/0/1243	
Goodness-of-fit on F^2	1.478	
Final R indices [I>2 sigma(I)]	R1 = 0.0797, wR2 = 0.2081	
R indices (all data)	R1 = 0.1208, wR2 = 0.2348	
Largest diff. peak and hole	2.545 and -2.969 e.$Å^{-3}$	

Table 4: Crystal data and structure refinement for compound **5**

Empirical formula	$C_{19}H_{19}Bi_{19}Cl_{19}P_{19}$
Formula weight	5479.94
Temperature/K	273.15
Wavelength	0.71073 Å
Crystal system	monoclinic
Space group	$P2_1/c$
Unit cell dimensions	a = 10.1384(15)Å α = 90°
	b = 16.087(3)Å β = 90.308(4)°
	c = 13.184(2) Å γ = 90°
Volume	2150.4(6)
Z	1
Density(calculated)	4.232
Absorption coefficient	39.673
F(000)	2318.0
Theta range for data collection	3.994 to 50.192
Index ranges	-11<= h <=12, -19<= k <=19, -15<= l <= 15
Reflections collected	33405
Independent reflections	3821
Completeness to theta	100%
Absorption correction	multi-scan
Max. and Min. Transmission	0.7452 and 0.6422
Refinement method	Full-matrix least-squares on F^2
Data/ restraints/ parameters	3821/0/244
Goodness-of-fit on F^2	1.569
Final R indices [I>2 sigma(I)]	R1 = 0.0595, wR2 = 0.2035
R indices (all data)	R1 = 0.0739, wR2 = 0.2126
Largest diff. peak and hole	3.480 and -2.695 e.Å^{-3}

Table 5: Crystal data and structure refinement for compound **6**

Empirical formula	CHAgBiClFOPS
Formula weight	463.35
Temperature/K	296.15
Wavelength	0.71073 Å
Crystal system	monoclinic
Space group	$P2_1/n$
Unit cell dimensions	a = 11.183(2)Å α = 90°
	b = 20.239(4)Å β = 91.289(5)°
	c = 21.578(5) Å γ = 90°
Volume	4882.5(18)
Z	24
Density(calculated)	3.782
Absorption coefficient	24.713
F(000)	4848.0
Theta range for data collection	2.76 to 50.232
Index ranges	-13<= h <=13, -24<= k <=24, -25<= l <= 25
Reflections collected	60531
Independent reflections	8686
Completeness to theta	99.60%
Absorption correction	multi-scan
Max. and Min. Transmission	0.7452 and 0.6319
Refinement method	Full-matrix least-squares on F^2
Data/ restraints/ parameters	8686/6/591
Goodness-of-fit on F^2	0.937
Final R indices [I>2 sigma(I)]	R1 = 0.0468, wR2 = 0.1234
R indices (all data)	R1 = 0.0771, wR2 = 0.1489
Largest diff. peak and hole	0.900 and -1.346 e.$Å^{-3}$